FINAL TECHNICAL REPORT: **BI-CONTINUOUS MULTI-COMPONENT NANOCRYSTAL SUPERLATTICES FOR SOLAR ENERGY CONVERSION**

DOE GRANT NUMBER: DE-SC0002158

APPLICANT/INSTITUTION/ADDRESS:

Cherie R. Kagan (PI)
Department of Electrical & Systems Engineering
Department of Materials Science & Engineering
Department of Chemistry
University of Pennsylvania
200 South 33rd Street
Philadelphia, PA 19104
Voice: 215-573-4384
Fax: 215-573-2068
e-mail: kagan@seas.upenn.edu

Christopher B. Murray
Department of Chemistry
Department of Materials Science & Engineering
University of Pennsylvania
231 South 34th Street
Philadelphia, PA 19104
Voice: 215-898-0588
Fax: 215-573-9711
e-mail: cbmurray@sas.upenn.edu

Jay Kikkawa
Department of Physics & Astronomy
University of Pennsylvania
209 South 33rd Street
Philadelphia, PA 19104
Voice: 215-898-7522
Fax:
e-mail: kikkawa@physics.upenn.edu

Nader Engheta
Department of Electrical & Systems Engineering
University of Pennsylvania
200 South 33rd Street
Philadelphia, PA 19104
Voice: 215-898-9777
Fax: 215-573-2068
e-mail: engheta@ee.upenn.edu

PRINCIPAL INVESTIGATOR:

Address:

Cherie R. Kagan
University of Pennsylvania
200 South 33rd Street
Philadelphia, PA 19104

Telephone Number: 215-573-4384
e-mail: kagan@seas.upenn.edu

DOE/OFFICE OF SCIENCE PROGRAM OFFICE: Materials Science and Engineering Division

DOE/OFFICE OF SCIENCE PROGRAM OFFICE TECHNICAL CONTACT: Dr. Michael Sennett

PROJECT PERIOD: 9/15/2009-9/14/2016

Program Scope: Our SISGR program studied an emerging class of nanomaterials wherein different combinations of semiconductor or semiconductor and plasmonic nanocrystals (NCs) are self-assembled into three-dimensional multi-component superlattices. The NC assemblies were designed to form bicontinuous semiconductor NC sublattices with type-II energy offsets to drive charge separation onto electron and hole transporting sublattices for collection and introduce plasmonic NCs to increase solar absorption and charge separation [**Fig. 1**]. Our group is expert in synthesizing and assembling an extraordinary variety of artificial systems by tailoring the NC building blocks and the superlattice unit cell geometry. Under this DOE BES Materials Chemistry program, we introduced chemical methods to control inter-particle distance and to dope NC assemblies, which enabled our demonstration of strong electronic communication between NCs and the use of NC thin films as electronic materials. We synthesized, assembled and structurally, spectroscopically, and electrically probed NC superlattices to understand and manipulate the flow of energy and charge toward discovering the design rules and optimizing these complex architectures to create materials that efficiently convert solar radiation into electricity.

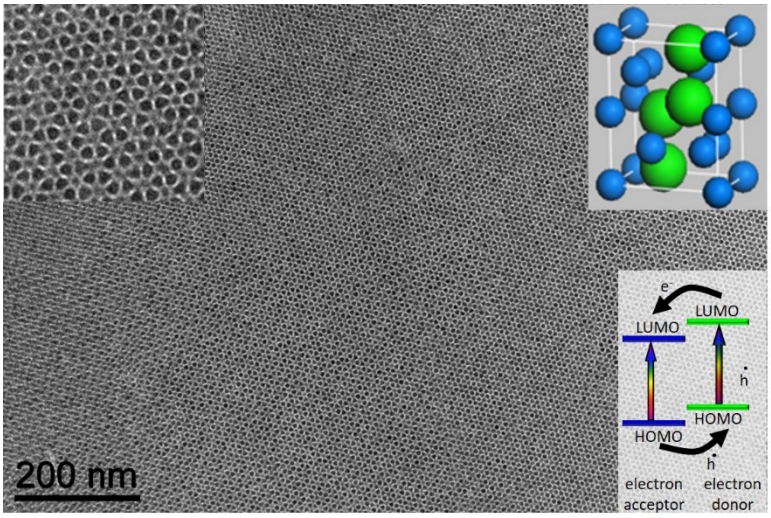

Fig. 1 TEM image of a binary nanocrystal superlattice at low resolution and (inset, left) high resolution of 8 nm CdTe:4 nm CdSe assembled in a $MgZn_2$ structure (inset, upper right). This NC assembly exemplifies materials studied to create a type-II energy offset and electron and hole transporting sublattices (inset, bottom right).

1. Synthesis of Semiconductor Nanocrystals

II-VI NCs - High-quality II-VI semiconducting NCs were synthesized by hot-injection methods[1,2] in the Murray group. Syntheses were tailored to achieve a high degree of monodispersity of particles and provide the widest possible range of sizes. This level of control is very important for assembly of NCs into ordered structures [**section 3]** and for optical and electrical characterization, as it reduces site-to-site dispersion of electronic levels within a NC film, allowing the fate of photoexcitations to be tracked spectroscopically (Kikkawa)[3] [**section 6**] and high mobility charge transport to be probed electrically (Kagan/Kikkawa)[4] [**section 7**]. These NC were also used as building blocks to demonstrate the first NC integrated circuits (Kagan)[5] [**section 8**].

By refining seeded growth techniques, CdSe/CdS dot-in-rod NCs of varying core and shell size and shape were synthesized by the hot injection of CdSe NC seeds into a reaction pot with precursors for the growth of CdS shells. By tuning the free ligands which are present in the reaction solution, in this case by introducing phosphonic acids, the shell was grown preferentially along the *c*-axis of hexagonal CdS. These dot-in-rod NC building blocks were used to explore the assembly of shape-engineered NCs and their optical anisotropy (Murray/Kagan) [**sections 3** and **5**].[6]

IV-VI NCs - Similarly high-quality, monodisperse IV-VI semiconducting NCs were also synthesized in the Murray group.[7,8] The Pb-chalcogenide NCs were used to demonstrate dip-coating of large-area superlattices[9] (Murray/Kagan) [**section 3**], to develop hybrid ligand engineering strategies to increase the carrier mobility-lifetime product for NC optoelectronic devices (Kagan) [**section 2]**, and the intentional control of non-stoichiometry to n- and p-dope NC assemblies[10,11] (Kagan) [**section 4**]. Early in the project these systems were studied for their photoconductivity in striped NC superlattices[12] and by FET measurements, wherein the observed ambipolar charge transport was exploited to realize the first discrete NC circuits.[13] These systems were subsequently used to probe the evolution in charge transport mechanisms with increasing carrier concentration and to design n-type and p-type NC materials for CMOS electronics and photovoltaics[14] (Kagan) [**sections 7** and **8**].

I-III-VI NCs – Chalcopyrites are a promising class of heavy-metal free semiconductors for solar photovoltaics, however synthesizing high quality chalcopyrite NCs has remained a challenge. We developed a synthesis of monodisperse chalcopyrite $CuInSe_2$ NCs using metal salt precursors and an air- and room-temperature-stable chalcogen source in selenium (IV) oxide. Careful elemental analysis shows this synthesis produces NCs that are nearly stoichiometric and STEM and high resolution TEM images show the NCs are tetragonal bypramidal in shape [**Fig. 2**]. X-ray diffraction measurements confirmed that samples had size dispersions < 8%. These tetragonal byprimidal $CuInSe_2$ NCs are promising building blocks for solar energy conversion, and their self-assembly and photoconductivity are described in **section 3**. This work was published in ACS Nano **7**, 4307 (2013).[15]

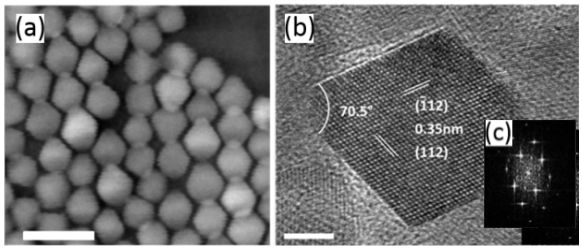

Fig. 2 STEM image of $CuInSe_2$ NC monolayer (scale bar 30 nm). (b) High-resolution TEM image (scale bar 5 nm) and (c) it's fast Fourier transform for a single NC.

2. Nanocrystal Ligand Exchange to Control Interparticle Distance and Coupling in the Solid State

We employed both small organic ligands (*e.g.* alkyl and aryl mono- and di- thiols, amines, and acids) and the more compact, inorganic ligands (*e.g.* chalcogenides, hydroxides, halides and the pseudohalide thiocyanate) that we, under the DOE program, and the community has introduced to exchange the long, insulating ligands commonly used in NC synthesis.[16–23] In particular the Kagan and Murray groups

collaboratively introduced the compact ligand thiocyanate, which provides short interparticle spacing and allows strong inter-particle coupling, which led to important breakthroughs in charge transfer and transport in the NC solid state [**Fig. 3**]. This work was published in the Journal of the American Chemical Society **133**, 15753 (2011). Solution-phase ligand exchange (prior to thin film deposition) with thiocyanate was used to prepare high mobility CdSe NC samples for optical and electrical measurements that probe the flow of excitations and carriers in strongly coupled NC systems [**sections 6** and **7**] and to demonstrate NC integrated circuits [**section 8**]. Solid-state ligand exchange (after thin film deposition) with the range of small organic and inorganic ligands was used to demonstrate high mobility n-type and p-type IV-VI NC thin films and enhanced power conversion efficiency in solar photovoltaics [**section 4**] and to explore the evolution from hopping to band-like transport with increased NC coupling and doping [**section 7**].

Fig. 3 (Left) Schematic of ligand exchange by treatment with NH_4SCN. (Right) Biphasic mixtures of hexane and DMSO with as-synthesized NCs on the left of each pair and NCs treated with NH_4SCN, washed, and re-dispersed in DMSO with hexane added on top on the right for: (left to right): Au, ZnSe, and CdSe NCs.

We also introduced a stepwise, hybrid ligand-exchange method for lead chalcogenide nanocrystal (NC) thin films using the compact-inorganic ligand thiocyanate (SCN) and the short-organic ligand benzenediothiolate (BDT). The compact SCN ligand is effective at reducing interparticle distance to yield high carrier mobility thin films, but a low surface coverage of SCN ligands generates a greater concentration of surface states.[24] The long length of BDT ligands creates NC thin films with relatively large interparticle distance and therefore low mobility and conductivity, but BDT passivates NC surface sites supporting long carrier lifetime.[25,26] By sequentially treating lead chalcogenide NC thin films with SCN and BDT [**Fig. 4a**], we increase both carrier mobility and lifetime by decreasing interparticle distance and passivating surface states. We systematically studied the effects of these ligands on the electronic and optoelectronic properties of NC thin films using spectroscopic and device measurements. Using this hybrid ligand exchange method, we successfully showed an enhanced mobility-lifetime product of majority carriers, enabling the demonstration of high-performance photoconductive photodetectors, and of minority carriers, resulting in improved efficiencies in photodiodes for light harvesting [**Fig. 4b**]. This work was published in Chemical Communications 53, 728 (2017).[27]

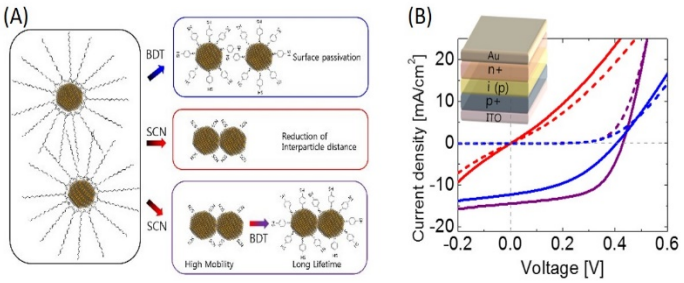

Fig. 4 (a) Schematic of (black) as-synthesized PbE (E=S, Se) NCs and ligand exchange with (blue) BDT, (red) SCN, and (purple) the hybrid SCN-BDT strategy used to enhance carrier mobility and lifetime in NC thin films. (b) I–V curves of PbS NC thin film solar cells treated with (blue) BDT, (red) SCN and (purple) SCN followed by BDT (dash line) in the dark and (solid line) under illumination.

3. NANOCRYSTAL ASSEMBLY AND PROCESSING

Murray and Kagan developed and employed a number of coating and assembly routes to integrate semiconductor NC thin films onto rigid and flexible substrates, allowing the realization of new structures and morphologies of NC superlattices, and the exploration of fundamental physical properties through a wide range of structural, optical, and electrical measurements.

Nanocrystal Membranes- The Murray group developed a novel and general method based on the liquid-air interfacial assembly of single and multi-component NCs to grow centimeter-scale, uniform superlattice and BNSL membranes that can be readily transferred to arbitrary substrates [**Fig. 5**].[28] Our method circumvents the limitations associated with the current assembly strategies, enabling integration of large-scale single-component superlattice and BNSLs on any substrate for the fabrication of NC-based devices.

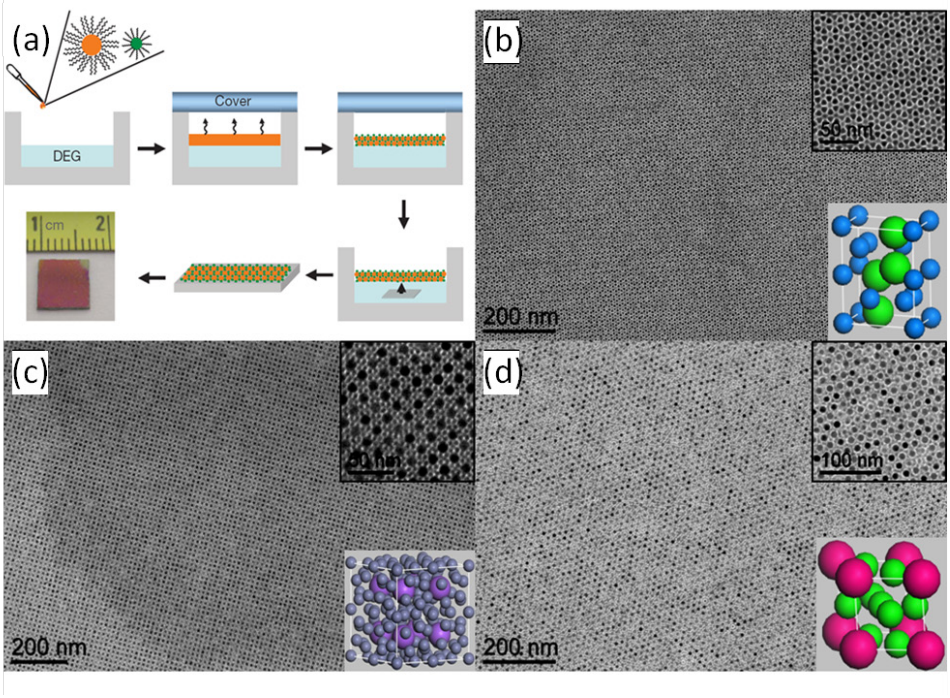

Fig. 5 (a) Schematic for the interfacial liquid-air assembly of BNSLs. NCs are mixed, dopcast onto a polar liquid, forming organized assemblies during slow evaporation, and are subsequenly transferred to arbitrary substrates. Bi-continuous BNSLs were formed in the (b) $MgZn_2$ phase form PbTe and PbS NCs, (c) $NaZn_{13}$ phase with PbSe and PbS NCs and (d) $CaCu_5$ phase with two different PbSe NC components.

The ability to transfer BNSLs also allows the construction of free-standing membranes and other complex architectures that have not been accessible previously.

Compared to the growth of single-component superlattices, the assembly process for BNSLs is more complicated, with a number of distinct pairwise interactions (van der Waals, dipolar, Columbic, etc) combining with hard sphere space-filling rules to drive the self-assembly of multi-component NCs. Existing methods to grow BNSLs rely on the evaporation of a binary NC solution on a solid substrate. Our method is based on drying-mediated self-assembly of multi-component NCs on an immiscible *liquid* surface, enabling the growth of macroscopic BNSL membranes with no substrate restrictions under ambient conditions. To grow BNSL membranes, a drop of hexane solution containing NCs with selected sizes and concentrations was spread over the surface (~ 1.5 × 1.5 cm^2) of diethylene glycol (DEG) in a Teflon well [**Fig. 5**]. The well was covered with a glass slide and hexane was then allowed to evaporate over 5-10 min, resulting in a solid film supported on the DEG subphase surface. To transfer BNSLs, a substrate was placed under the floating film and then gently lifted up. In this way, centimeter-scale BNSL membranes can be readily transferred to the substrate after drying. In a typical assembly process for an AlB_2-type BNSL membranes consisting of 11-nm PbS and 5-nm PbSe NCs, 10 µL hexane solution of PbS NCs (~ 6 mg/mL) is mixed with 10 µL hexane solution of PbSe (~ 3 mg/mL) NCs in a vial. The mixed NC solution was then spread on the surface of DEG in a Teflon well (~ 1.5 × 1.5 × 1.5 cm^3) and allowed to slowly evaporate

forming a solid membrane in 5-10 min. **Fig. 5(b-d)** show representative BNSLs formed by the membrane transfer process by mixing different combinations of Pb-chalcogenide NC compositions and sizes to form different BNSL structures.

The ability to transfer BNSLs also allows the construction of unique architectures such as free-standing membranes, which are ideal structures to fabricate devices free of substrate-induced interference. **Fig. 6** shows a free standing BNSL membrane and highlights the organization of the two NC components at an unzipping along the structure. The ability to transfer NC superlattices and BNSLs enables the fabrication of NC-based devices as well as complicated architectures, which we utilize in our measurements below, and will accelerate the exploration of this new and important class of materials. As a demonstration of the potential for these techniques to produce device-scale films, we recently used the membrane assembly method to fabricate the active layer of single-component PbS nanocube films for circuits on flexible plastic substrates.[13]

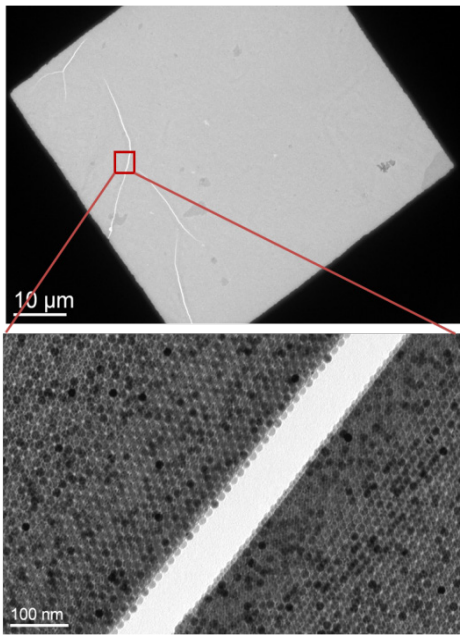

Fig. 6 TEM image of free standing BNSL membrane. Highlight along the crack, the unzipping of the two ordered NC components is seen.

Nanocrystal Stripes **-** In contrast to the slow drying of NC dispersions on the immiscible liquid interface to form smooth NC superlattices and BNSLs, described above, we found on this immiscible liquid interface an unusual, yet universal dynamic assembly phenomenon that enables the formation of centimeter-scale, periodically ordered stripe structures of NC superlattice films that form quickly within 15 sec.[12] Our method is based on a far-from-equilibrium assembly process that occurs during the rapid drying of a NC dispersion, for example of NCs in alkanes on an immiscible polar organic subphase, that is general for NCs of different size and shape and is similarly compatible with the transfer and integration of striped NC superlattice films on

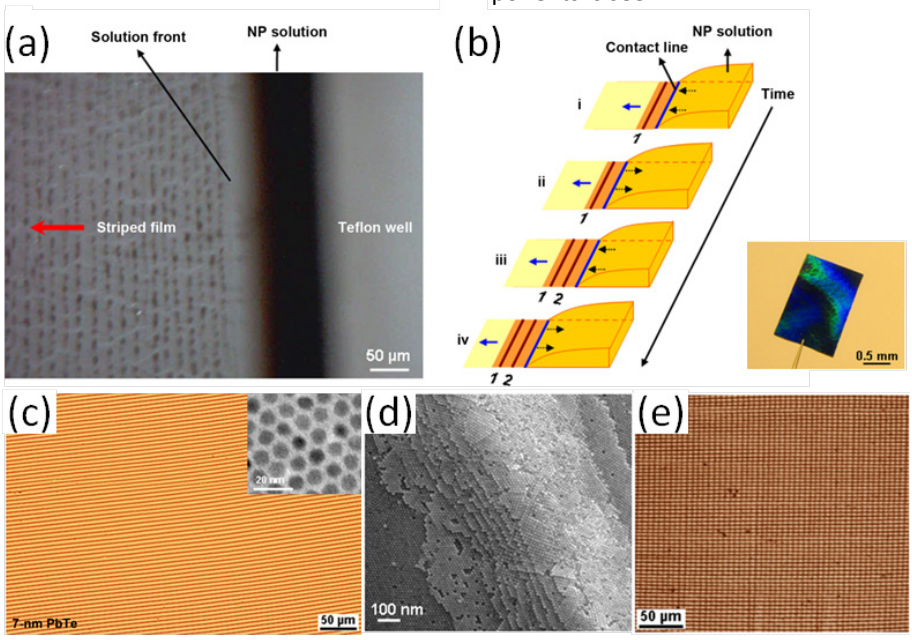

Fig. 7(a) Snapshot of striped NC superlattice formation growing from the solution front at the subphase edge. Red arrow indicates the film sliding direction. (b) Proposed mechanism of pattern formation, showing the oscillatory motion of the contact line at the subphase edge inducing the stripe formation. The first- and second formed stripes, labeld by "1" and "2" and arrows to represent sliding motion. (inset) Photo of striped film composed of 10 nm Fe_3O_4 NCs transferred to a SiO_2/Si wafer showing the film iridescence. (c) Photo of striped 7 nm PbTe NC superlattice and inset, the TEM micrograph of the component PbTe NCs. (d) SEM micrograph highlighting a single ridge of a NC stripe. (e) Multilayer films formed by sequentially transferring two striped films of 6 nm FePt NCs in orthogonal directions.

arbitrary substrates. **Fig. 7(a)** shows a snapshot as the striped NC structure emanates from solution at subphase edge. The highly periodic stripe pattern is formed by a novel contact-line instability, as depicted schematically in **Fig. 7(b)**. The periodic NC superlattices formed on the liquid subphase are readily transferred to substrates as shown by the inset. **Fig. 7(c)** shows an example of the striped NC membranes composed of PbTe NCs. The stripes formed are of uniform height and pitch (as we have shown by AFM) and remain well ordered, as seen in the SEM image [**Fig. 13(d)**]. The thickness of the ridges consist of terraced NC superlattices varying between 2 and 10 NC layers (depending on the concentration and volume of the NC dispersion), while the underlying film can be adjusted from monolayer, bilayer, to multilayer. The periodicity of the stripes is tunable at micron scales by varying the NC concentration. The ability to transfer the membranes to substrates allows us to stack these stripes NC membranes on substrates. For examples, **Fig. 7(e)** shows two NC striped membranes stacked orthogonally. The design of NC structures on multiple length scales opens an exciting avenue for the large area design of NC materials for devices and we have used these architectures to probe structuring NC absorbers for photoconductivity [**Section 6**]. This work was published in Nano Letters **11**, 841 (2011).

Assembly of Shape-Engineered NCs – Deposition of NC dispersions on both solid (drop-cast) and liquid interfaces were used to assemble shape-engineered NC superlattices. For example, the tetragonal byprimidal $CuInSe_2$ NCs self-assembled into three-dimensional, ordered arrays upon drop-casting dispersions. **Fig. 4** shows a TEM image highlighting the face-to-face packing of NC facets and inset, the selected-area wide-angle electron diffraction reflects the single-crystalline assembly. SEM imaging shows this ordering of the NCs extends through the three-dimensional volume of the film [**Fig. 8**] [Published in ACS Nano **7**, 4307 (2013)].[15] These shape-engineered NC assemblies allow high-density packing of NCs to fill space and are photoconductive, introducing desirable target NC building blocks that utilize the three-dimensional volume of the film for high absorptivity and that have large interfacial areas and crystallinity for high mobility transport.

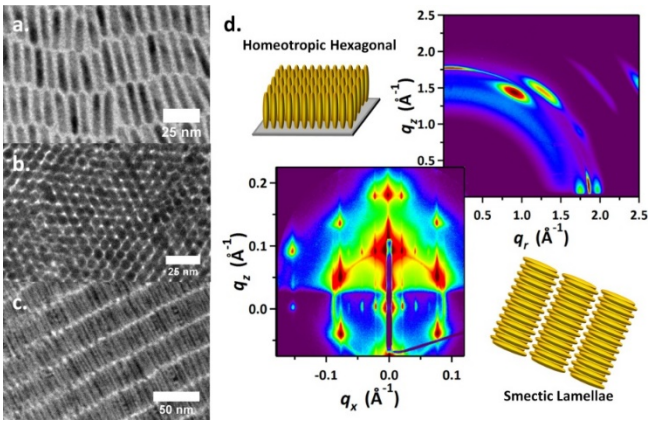

Fig. 8 TEM image of (a) a colloidal dot-in-rod sample. Assembly of the nanorods on (b) diethylene glycol and (c) water subphases. (d) Schematic of homeotropic ordering [seen in (b)] and smectic ordering [seen in (c)] and example small- and wide-angle x-ray scattering measurements used to provide a complete description of interparticle ordering and a quantitative description of nanorod alignment in three dimensions.

Shape-control was further exploited by using monodisperse colloidal dot-in-rod nanorods to self-assemble large-area smectic, liquid-crystalline superlattices.[29] Using the liquid-interfacial self-assembly technique, but varying the liquid subphase used for self-assembly allows the orientation of nanorod superlattices to be tuned from nearly complete vertical alignment to nearly complete horizontal alignment [**Fig. 8**]. We show that the surface tension of the subphase is strongly correlated with the orientational ordering of the nanorod superlattices. Detailed structural studies using grazing-incidence small-angle x-ray scattering (GISAXS) and grazing-incidence wide-angle x-ray scattering (GIWAXS) measurements revealed that the crystal axes of individual nanorods are co-aligned along specific zone axes of the superlattice assembly.

We probed the optical properties of individual superlattices in different orientations by measuring and mapping the polarization-dependent photoluminescence by confocal techniques. Polarized excitation measurements were correlated with real space imaging of the same spots by electron microscopy. Vertically-aligned superlattices show no in-plane polarization [**Figs. 9a,b**]. However, the excitation of horizontally-aligned nanorod superlattices showed large optical anisotropy aligned along the nanorod long axes. [**Figs. 9c,d**]. This work demonstrates that the unique optical properties of isolated NCs can be preserved and collectively directed in long-range superlattices and oriented with respect to the substrate. The orientation of transitions dipoles and polarization control in anisotropic NC building blocks promises a route to control the flow of energy and excitations in single and multi-component NC superlattices. This work was published in Chemistry of Materials **27**, 2998 (2015).[6]

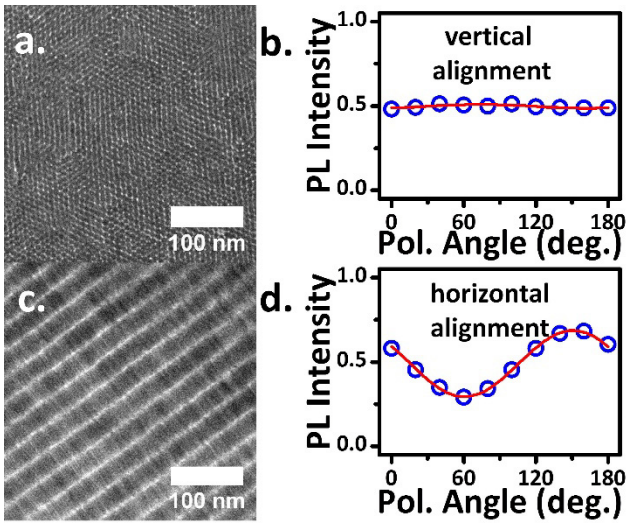

Fig. 9 (a) Vertically aligned nanorod array and (b) corresponding polarized excitation PL measurement from the same spot, as a function of polarizer angle. (c) Horizontally-aligned nanorod superlattice with the corresponding polarized excitation measurement (d).

Quasicrystalline nanocrystal superlattices with partial matching rules **-** We worked to expand the library of self-assembled superstructures and provide insight into the behavior of atomic crystals and support the development of materials with mesoscale order. We built on recent findings of soft matter quasicrystals and reported a quasicrystalline binary nanocrystal superlattice that exhibits correlations in the form of partial matching rules reducing tiling disorder. We determined a three-dimensional structure model through electron microscopy [**Fig. 10**], electron tomography and direct imaging of surface topography. The 12-fold rotational symmetry of the quasicrystal was broken in sublayers, forming a random tiling of rectangles, large triangles and small triangles with 6-fold symmetry. We analyzed the geometry of the experimental tiling and discuss factors relevant for the stabilization of the quasicrystal. Our joint experimental–computational study demonstrated the power of nanocrystal superlattice engineering and further narrowed the gap between the richness of crystal structures found with atoms and in soft matter assemblies. This work was published in Nature Materials **16**, 214-220, (2017).[30]

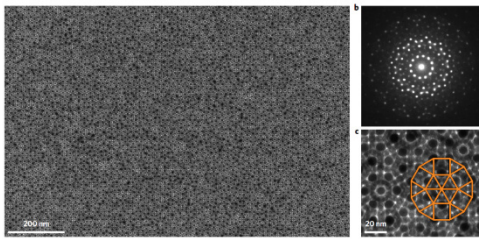

Fig. 10 Self-assembled binary NC superlattices with quasiperiodic and periodic order. a–c, Low-magnification TEM image (a), SAED pattern (b) and high-magnification TEM image (c) of a dodecagonal quasicrystal self-assembled from 6.8nm CoFe2O4 and 12.0nm Fe3O4 NCs. d,e, Low-magnification TEM image and SAED pattern (inset).

Large-area dip-coating of Single and Multi-Component Nanocrystal Superlattices - We showed that dip-coating, a desirable method for NC thin film deposition, could be used to assemble ordered, single- and multi-component NC superlattices. These NC superlattices are polycrystalline and can be deposited over arbitrarily large wafer scales. For example, we showed a PbSe NC superlattice deposited over 100 mm substrates. The dip-coating technique was extended to deposit other single component superlattices, from spherical NCs of Bi and $CoFe_2O_4$ and cubes of $MnFe_2O_4$, and to binary nanocrystal superlattices

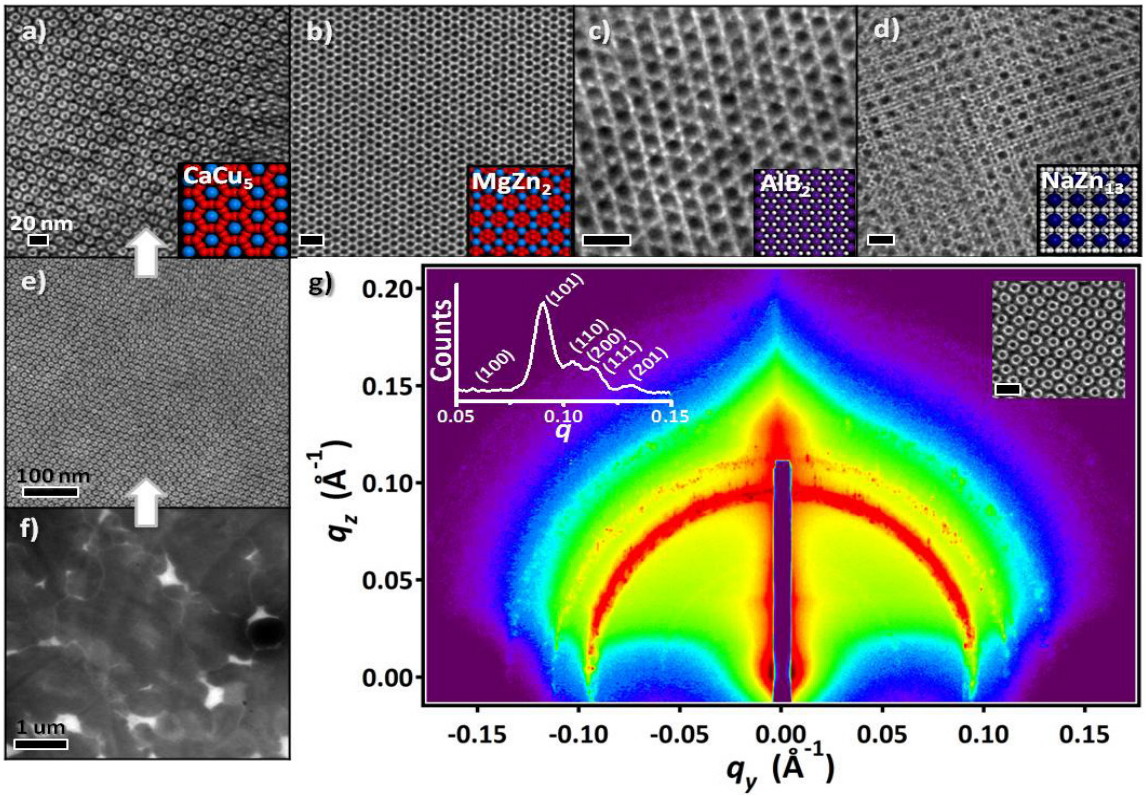

Fig. 11 Dip-coated BNSL assemblies of: 5.4 nm PbSe and 3.4 nm PbS (a) in a $CaCu_5$ structure and (b) in a $MgZn_2$ structure, (c) 8.2 PbSe and 3.4 nm PbS in an AlB_2 structure, and (d) 8.4 nm PbSe and 3.4 nm PbS in an $NaZn_{13}$ structure. Scale bars are 20 nm. (e, f) Lower magnification images of the $CaCu_5$ structure. (g) GISAXS of $CaCu_5$ structure with insets of transmission SAXS (left) and higher resolution TEM (right) [scale bar: 20 nm].

(BNSLs). Dip-coating allowed the formation of BNSLs having different unit cell geometries, including $CaCu_5$, $MgZn_2$, AlB_2, and $NaZn_{13}$, structures, exemplified by assemblies constructed from different sizes and molar ratios of PbS and PbSe NC building blocks [**Fig. 11a-d**]. Grain sizes are typically ~0.25-5 μm^2 in size [**Fig. 11e,f**] and the structure is consistent over the entire substrate as shown by GISAXS measurements [**Fig. 11g**].

Fig. 12a shows a BNSL film dip-coated onto a silicon wafer, demonstrating the arbitrarily large areas over which the films can be deposited onto a device relevant substrate. SEM images of the wafer confirm formation of the $MgZn_2$ structure from PbS and PbSe NCs [**Fig. 12b-d**]. Scale up is necessary for comprehensive studies of the optical and electrical properties of BNSL films. Having films deposited onto arbitrarily large substrates allows for device statistics on a single film. Furthermore, many substrates can be rapidly coated in sequence from

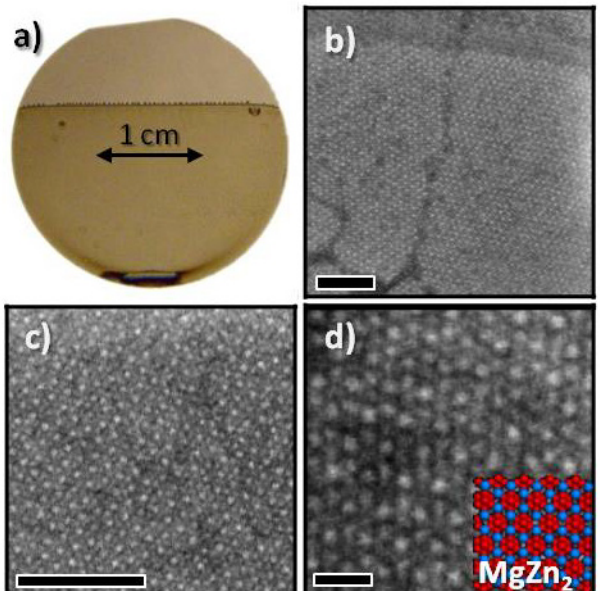

Fig. 12 (a) Photograph of a 25 mm wafer dipped into a co-dispersion of PbSe and PbS NCs. SEM images showing a polycrystalline $MgZn_2$ phase BNSL. Scale bars are 100 nm for (b, c) and 20 nm for (d).

the same stock solution, or one film can be processed through multiple steps, such as ligand exchange and solvent rinse, using our computer automated system. The work was published in Advanced Materials, **27** 2846 (2015).[31]

4. Doping Nanocrystal Assemblies

Early in the project we demonstrated that semiconductor NCs could be doped by introducing extrinsic atoms at their surface ("remote doping") through thermal evaporation and diffusion to form CdSe NC thin films with high electron mobilities of μ_n~27 cm^2/Vs[32] or by oxygen adsorption on PbSe nanowires with hole mobilities of μ_p~9 cm^2/Vs.[33] We have expanded methods to control the atoms at the surface of NCs and therefore to remotely dope NC thin films.

Stoichiometric Control to Design NC Thin Film Electronic and Optical Properties - The electronic properties of bulk or thin film II-VI and IV-VI semiconductors are known to be greatly influenced by their stoichiometry. Kagan and Murray showed that we could tailor the stoichiometry of IV-VI NC thin films and therefore the carrier type, concentration and mobility.[10] As-synthesized and thiocyanate exchanged PbSe and PbS NC thin films show ambipolar characteristics in FETs with electron and hole mobilities of $\leq 10^{-2}$ cm^2/Vs. However, from device-to-device predominant electron or hole transport often arises from unintentional n-doping as syntheses typically yield Pb-rich NCs[34] or p-doping from oxygen adsorption even at the <0.1 ppm levels in nitrogen glovebox.[35–37] In the first example, we applied thermal evaporation and diffusion of metal (Pb) and chalcogen (Se) to intentionally and controllably dope lead chalcogenide (PbSe and PbS) NC thin films from intrinsic to n-type (with excess Pb) and p-type (with excess Se) [**Fig. 13a**]. Increasing the Pb or Se deposition allowed us to tailor the electron and hole concentration from near intrinsic at 10^{15} carriers/cm^3 to degenerately n- or p-doped at 10^{20} carriers/cm^3, thus positioning the Fermi level position throughout the NC thin film bandgap [**Fig. 13b**]. Capacitance-voltage in combination with Hall measurements (not shown) were used to characterize the tunability in electron and hole concentrations by intentional Pb- and Se-enrichment. By controlling the stoichiometry we demonstrated lead chalcogenide NC FETs to be ambipolar, n-type or p-type. In particular, we demonstrated μ_n~ 10 cm^2/Vs with excess Pb in PbSe NC FETs, an order of magnitude higher than lead chalcogenide devices that had been reported [**Fig. 13c**]. We also showed that we could use non-stoichiometry to control the junctions of devices, exemplified by enhanced power conversion efficiency in Se-doped PbSe Schottky junctions [**Fig. 13d**]. This work was published in ACS Nano **7**, 2413 (2013)[10] and highlighted in an *ACS Nano Perspective* written by Luther (NREL) and Pietryga (LANL).[38]

We extended these ideas of remote doping to develop a post-synthesis, solution-based colloidal atomic layer deposition process to introduce adatoms at the NC surface [**Fig. 14**].[11] This stepwise method controls carrier statistics and therefore electronic properties. Starting with lead chalcogenide NCs, we (a) deposit

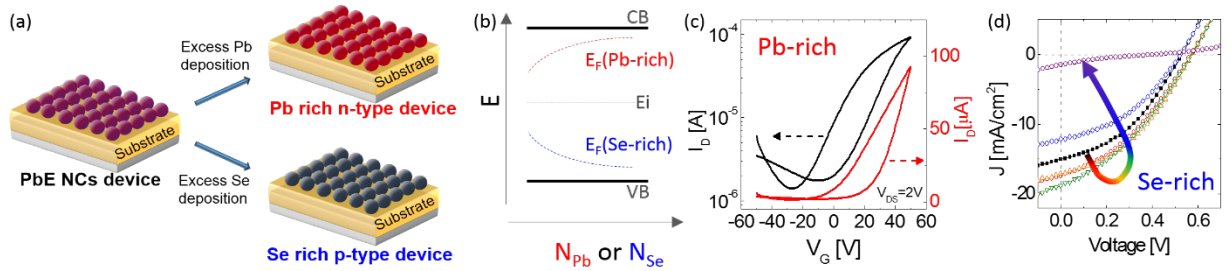

Fig. 13 (a) Schematic of stoichiometric control of PbE (E=S, Se) NC thin films by Pb or Se enrichment. (b) Fermi energy of PbE NC thin films as a function of Pb (red) and Se (blue) enrichment. (c) Transfer characteristics of a PbSe NC FET in the linear regime upon enrichment by 3 Å of Pb deposition. (d) Current-density voltage characteristics of PbSe NC solar cells (black) before and after enrichment by (red) 0.1 Å, (orange) 0.2 Å, (green) 0.4 Å, (blue) 0.8 Å, and (purple) 2 Å of Se deposition.[10]

NCs with their long-ligands, producing NC thin films with a hexagonal structural motif that are electrically insulating. Exchange of these ligands using chalcogenide salts [*e.g.* Na_2Se, Na_2S or KHS], (b) enriches the NC surface in the chalcogen,[22] creating high energy surface states that drive NC fusion on {100} facets and structurally transforms the films into ordered NCs in a cubic motif, akin to reports of ligand stripping.[39,40] We showed these chalcogen-rich NC films have a high density of trap states, are oxygen sensitive, and show heavily p-type charge transport. Further treatment with $PbCl_2$ (c) converts these to n-type films by enriching the NCs in Pb, maintains the cubic structure, and passivates the NC surfaces to form stable materials. This process and the resulting films were characterized by a wide range of structural, analytical, optical and electrical measurements. For example, **Fig. 14d** shows the optical properties of (black) as-synthesized NC thin films and films exchanged with (blue) the chalcogenide salt. The absorption red-shifts due to NC fusion and the addition of chalcogen atoms at available Pb-sites, and broadens due to midgap states introduced by surface chalcogens and oxygen adsorption. (red) Pb-enrichment at surface chalcogen sites gives rise to a further red shift, but narrowing of the excitonic transitions as the metal passivates surface states [**Fig. 14e**]. This process is general for S- and Se-enrichment and subsequent Pb-enrichment of PbS and PbSe NC thin films. **Fig. 14f** shows the electrical properties of lead chalcogenide NC thin films treated by colloidal atomic layer deposition. (blue) Chalcogen-rich NC thin films show heavy p-type transport, however upon increased Pb-enrichment (green, orange, red), the NC FETs become increasingly n-type. This solution-based method yielded n-type NC FETs with μ_n=4.5 cm^2/Vs, of similar order to that realized by doping through thermal evaporation and diffusion. This work was published in Nano Letters **14**, 1559 (2014).[11]

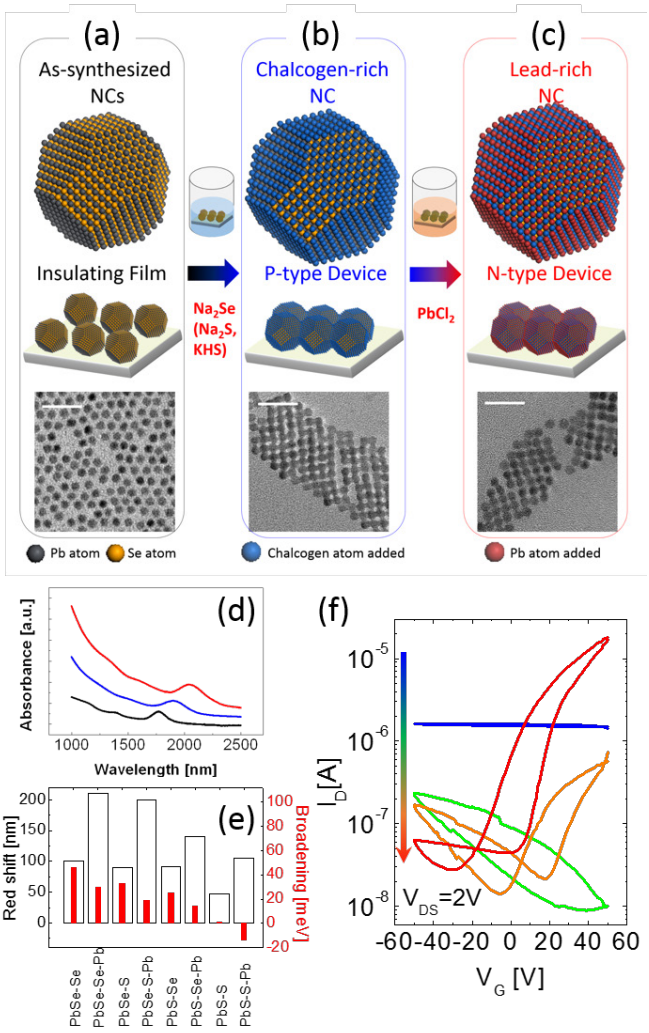

Fig. 14 (a-c) Schematic of post-synthesis, colloidal atomic layer deposition and structural characterization by TEM**.** Scale bar: 20 nm (d) Absorption spectra of as-synthesized PbSe NC thin films (black) and upon Se (blue) and Pb (red) enrichment. (e) Red shift and broadening in the absorption spectra of PbS and PbSe NC thin films upon S- or Se-enrichment and Pb-enrichment. (f) Transfer characteristics of Na_2Se treated PbSe NC thin films before (blue) and after $PbCl_2$ treatment for 1h (green), 6 h (orange) and 12 h (red) at 65˚C.

5. Structural and Optical Characterization of Nanocrystal Solids

X-ray diffraction - The structural characterization of NCs and their assemblies are presented throughout the proposal. However, here we highlight x-ray diffraction techniques Murray and Kagan developed to describe the purity, surface coverage, crystallinity, and grain size important to characterizing self-assembled, polycrystalline NC superlattices.[41] Grazing-incidence diffraction, shown in **Fig. 8** and **Fig. 11**,

reveals ordering over large areas. We also performed transmission X-ray diffraction measurements to interrogate the in-plane structure of NC superlattices with spatial resolution close to the grain size of superlattices.

We demonstrated that transmission measurements with a microfocused X-ray source [**Fig. 15a,b**] yield statistical information about superlattice grain size and size distribution. As demonstrated in **Fig. 15c,d**, polycrystalline superlattice films can be fabricated with average grain areas exceeding 100 μm^2, consisting of 10^7 individual NCs. Within this size regime, direct comparison of grain sizes can be made using X-ray diffraction and real space imaging by SEM; both give very similar average values [**Fig. 15b,d**]. Much larger grain sizes, consisting of $>10^9$ individual NCs, have subsequently been fabricated in CdSe and PbSe NC films, although in this case the grain size can no longer be measured by SEM. X-ray mapping experiments with 50 µm resolution across several square millimeters were performed to confirm that superlattice structure is preserved over much larger areas than those which can be imaged by electron microscopy. This technique was also applied to map polymorphism and the variation of superlattice orientation across large film areas. These methods were demonstrated on metal oxide (e.g. $CoFe_2O_4$), metallic (e.g. Au), semimetallic (e.g. Bi), and semiconducting (e.g. CdSe/CdS) NCs self-assembled into single-component, binary, and anisotropic superlattices. By correlating the small- and wide-angle scattering signals from identical spots, the preferential alignment of NCs within superlattices can be determined. This work was published in ACS Nano **8**, 12843 (2014).[41]

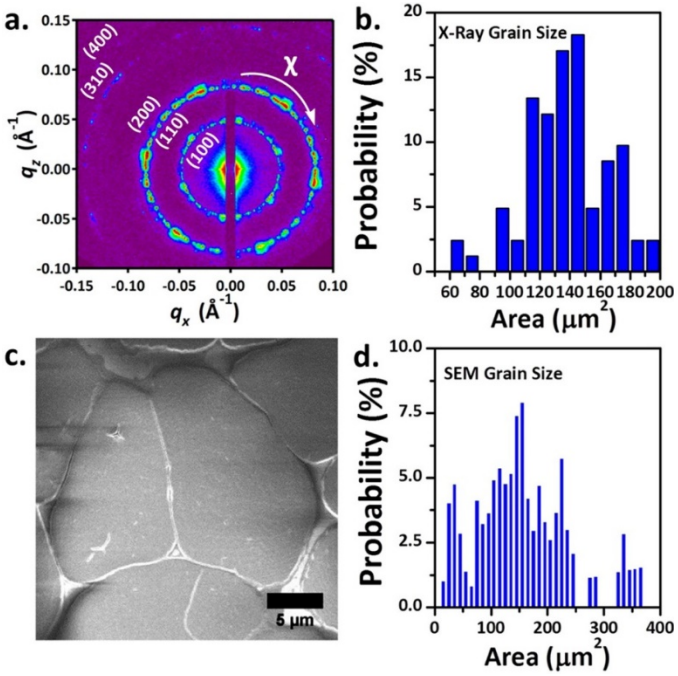

Fig. 15 (a) Grazing-incidence small-angle x-ray diffraction measurements of a Fe_3O_4 NC superlattice thin film. (b) Grain size distribution based upon x-ray measurements. (c) SEM image of a polycrystalline superlattice thin film analyzed in (b) with the grain size distribution in (d).

Statistical Description of CdSe/CdS Dot-in-Rod Heterostructures Using Scanning Transmission Electron Microscopy - We used annular dark-field scanning transmission electron microscopy (ADF-STEM) to provide a statistical description of the faceting, core location, stacking faults, and polar self-assembly behavior of CdSe/CdS dot-in-rod heterostructures described in **sections 3** and **5**. Applied to dot-in-rod and rod-in-rod heterostructures, STEM enables statistical measurements of core locations that show that the position of the CdSe core lies at ≈45% of the length of the sample, slightly closer to the blunt (001) facet of the CdS nanorod shell. A study of stacking faults reveals a substantially enhanced probability near the epitaxial interface of the core and shell, suggesting the role of epitaxial strain in the formation of defects. Structural analysis is extended to liquid-crystalline monolayers of nanorods, and the role of dipolar interactions within lamellae is analyzed using one-dimensional pair-distribution analysis of polarity, showing that the nanorods have a random dipole alignment. This work was published in Chemistry of Materials, **28** (10), 3345–3351 (2016).[42]

Spectrally-Resolved Dielectric Functions of Solution-Cast Quantum Dot Thin Films - Quantum confinement is the divergence, at small crystallite size, of the electronic structure of semiconductor nanocrystals, or quantum dots, from the properties of larger crystals of the same materials. Although the

extinction properties of quantum dots in the dispersed state have been extensively studied, many applications for quantum dots require the formation of a solid material which nonetheless retains a size-dependent electronic structure. The complex index of refraction (or complex dielectric function), including the extinction coefficient, is critical information for interpretation of optoelectronic measurements and use of quantum dot solids in optoelectronic devices. We used spectroscopic ellipsometry to provide an all-optical method to determine the thickness, complex index, and extinction coefficient of thin films made of quantum-confined materials through the visible and near-infrared spectral ranges [**Fig. 16**]. The characteristic, size-dependent spectral features in the absorption of monodisperse quantum dots are readily translated into spectral variations of the index of refraction. The complex indices of refraction of CdSe and PbS quantum dot solids depend strongly on quantum dot size and the processing conditions of the thin film, including ligand exchange and annealing. The dielectric functions of quantum dot solids are dominated by the fill fraction of quantum dots, with only secondary influence from interparticle interaction. This work as published in Chemistry of Materials, **27**, 6463–6469 (2015).[43]

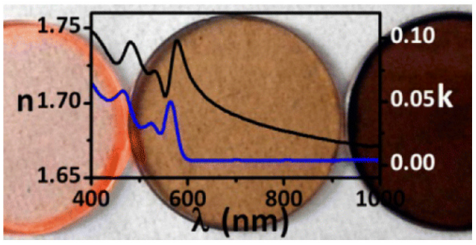

Fig. 16 Plots of n & k vs for CdSe closepacked films.

6. Excitonic Behavior and Charge Separation in Nanocrystal Solids

Shape-dependent Optical Anisotropy in Dot-in-Rod Nanocrystals - Colloidal nanorods represent one of many possible NC morphologies that can be used as a building block to diversify the phase space of binary assemblies. From the perspective of energy generation and transformation, semiconductor nanorods have several attributes distinctive from spherical quantum dots, in particular a polarized electronic structure and, in core-shell nanorods, carrier-selective delocalization. We have studied the polarization-dependent properties of colloidal nanorods and nanostructures reported in a series of publications.[44,45]

In earlier work, we developed methodologies to analyze the anisotropic optical properties of ensembles of colloidal nanorods and to quantify the degree of optical anisotropy of the electronic structure in nanorods and nanoplates.[46] These measurements indicated that shape-dependent optical anisotropy in anisotropic colloidal NCs is not readily predicted on the basis of far-field dielectric properties, but instead emerges from quantum confinement of electronic levels in one or two dimensions. These methods were subsequently extended to understand the optical properties of colloidal core/shell nanostructures.[44,45] Within a series of core/shell structures with anisotropic NC shells, subtle changes in the degree of local anisotropy about the emissive core material dramatically affect the oscillator strengths of different polarized excitations [**Fig. 17**]. The aspect ratio of the dot-in-rod structure is not strongly related to the degree of anisotropy, but *local anisotropy* of the anisotropic shell about the emissive core material drives higher polarization of the electronic structure. Samples which have much thicker shells showed lower anisotropy because the local environment at the CdSe core is relatively more isotropic than those samples with thin shells. Linear anisotropy is expressed in the relative strength of linearly-polarized transitions (0 change in angular momentum) compared to those which are circularly-polarized (±1). This work was published in J. Phys. Chem. Lett. **5**, 85 (2014).[44]

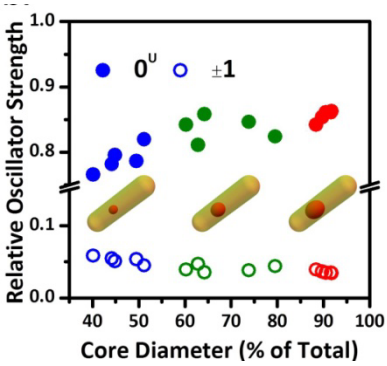

Fig. 17 Oscillator strength of linear polarization (0) and circular polarization (±1) in the band-edge electronic structure of colloidal dot-in-rod heterostructures as a function of the fractional core diameter.

Additional temperature- and time-resolved photo-luminescence measurements of dot-in-rod and rod-in-rod samples showed that the geometry of the heterostructure can be manipulated to enhance thermal stability. In contrast to previous works, it was unambiguously determined that ligand decomposition is not the primary mechanism of thermal instability of semiconductor NCs at elevated temperatures.[45] **Fig. 18** shows four samples of dot-in-rod and rod-in-rod CdSe/CdS heterostructures: each shows thermal redshift, homogeneous broadening, and decreased (but reversible) intensity heating to 600 K. It was found that samples with a larger core volume fraction preserved substantially more photoluminescence at elevated temperatures. Time-resolved studies showed that by tuning the core volume fraction of the core/shell NCs, the radiative recombination rate could be adjusted from <5 ns to >30 ns. Those samples which showed faster radiative recombination rates were substantially more stable against the onset of non-radiative recombination at elevated temperatures, resulting in enhanced thermal stability of photoluminescence and providing a route to engineer the exciton lifetime through materials design. This work has been published as *ACS Nano* **8**, 6466 (2014).[45]

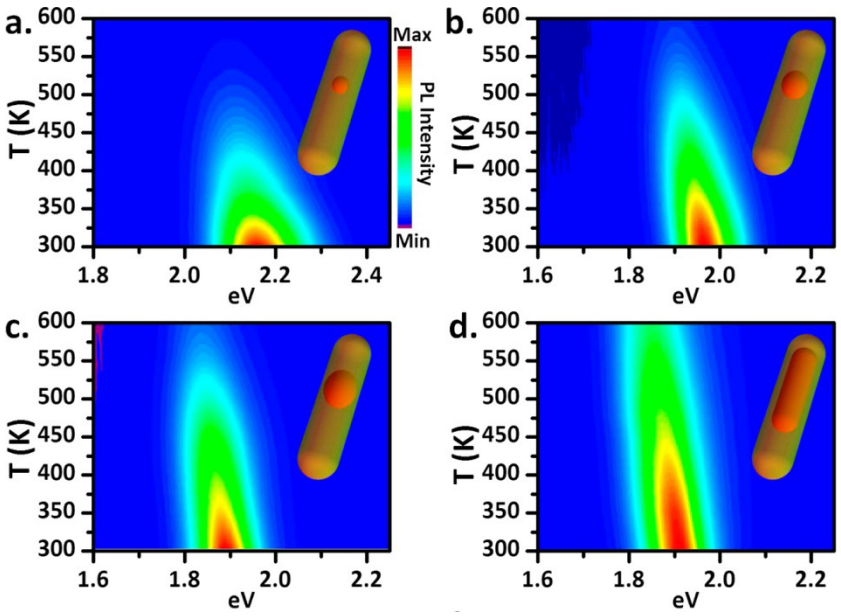

Fig. 18 (a-d) Temperature-dependent photoluminescence collected for dot-in-rod (a-c) and rod-in-rod CdSe/CdS (d) samples.

Ultrafast Electron Trapping in Ligand-Exchanged Nanocrystal Solids - Kikkawa, Kagan and Murray used ultrafast optical spectroscopy to study the evolution of core-surface interactions with ligand exchange and annealing in CdSe NC solids.[3] This work employed a unique, custom-made system designed to study time-resolved absorption (TRA) and time-resolved PL (TRPL) in NCs over a broad spectral range with sub-picosecond time resolution [**Fig. 19**]. We found that (a) exchanging aliphatic native ligands (NL) for thiocyanate (SCN) and subsequently annealing the samples to 200°C [Ref.[47]] drastically increases the rate of electron trapping to the NC surface and (b) assumptions widely made in the literature regarding TRA in CdSe NC systems were shown to be incorrect in this case.

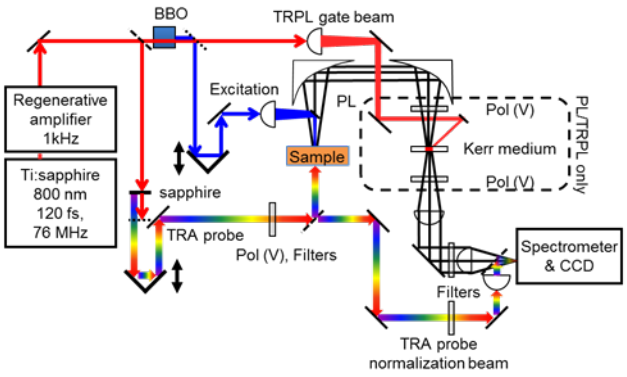

Fig. 19 Custom-built system for measuring broadband time-resolved PL and time-resolved absorption using the Kerr gate effect (TRPL) and a supercontinuum probe (TRA).

Fig. 20a-c shows a progressive decrease in band-edge PL lifetimes in CdSe NC solid films upon exchange and annealing. Time-integrated PL (not shown) shows a corresponding loss in band-edge quantum yield,

implicating an increase in non-radiative recombination and/or surface trapping with exchange and annealing.

Complementary TRA measurements indicate that electron trapping is responsible for PL lifetime decreases. TRPL measures the $1S_{3/2h}$-$1S_e$ exciton lifetime, so the longer lifetime of the aggregate $1S_{3/2h}$-$1S_e$ (B1) TRA bleach [**Fig. 20**] cannot be due to the exciton, but must instead arise from $1S_e$ electrons or $1S_{3/2h}$ holes within the NC core. Dynamics of the aggregate $2S_{3/2h}$-$1S_e$ (B2) TRA bleaches echo that of TRPL [**Figures 20d-f**], indicating that both capture $1S_e$ population decays. Thus, we find that *electron* trapping increases upon exchange and annealing, which is both surprising and informative. It may be the case that ligand decomposition upon annealing results in a CdS shell, which then assists hole trapping through a quasi-Type-II band alignment.[48,49] It is also possible that midgap states observed in our cyclic voltammetry measurements of annealed samples[50] introduce electron traps.

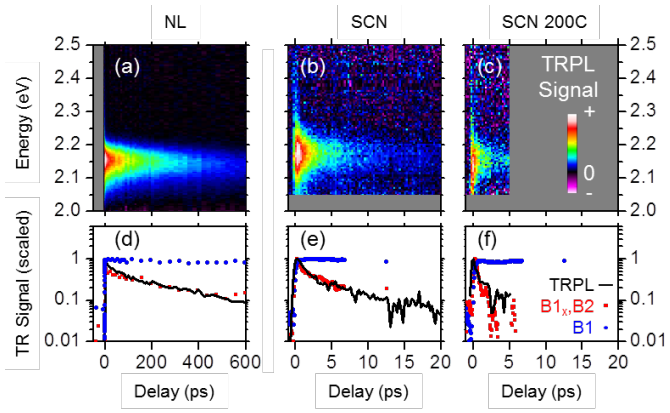

Fig. 20 Time-resolved PL of CdSe QD thin films (a) with native ligands (NL), (b) after ligand exchange with SCN, and (c) after ligand exchange and subsequent annealing at 200 °C. (d-f) compares TPRL (black) and TRA (red, blue) decays for the three samples. TRA population bleaches at the $1S_{3/2h}$-$1S_e$ (B1) and $2S_{3/2h}$-$1S_e$ (B2) transitions appear in blue circles and red squares, respectively. The exciton-resolved $1S_{3/2h}$-$1S_e$ bleach ($B1_x$) has the identical time evolution as TRPL, as expected, and is also shown in red.

The implication that the long-lived B1 bleach measures $1S_{3/2h}$ holes that persist subsequent to electron trapping runs counter to the widespread assertion that B1 quantifies $1S_e$ electron populations.[51–54] In this project, we further demonstrate theoretically that *either* $1S_e$ or $1S_{3/2h}$ produce strong B1 TRA bleaches at all temperatures from 10 K to 300 K. This work was published in ACS Nano, **9**, 1440 (2015).[3] These techniques were also applied to understand hot carrier luminescence that outcompetes slow vibrational relaxation in two-dimensional organic-inorganic metal-halide perovskites [published J. Am. Chem. Soc.].[55]

Large Photoconductivities in Thiocyanate Capped NC Thin Films - Interparticle spacing dramatically affects the strength of cooperative interactions between the NCs in the solid state and the rate of carrier transfer. Using NCs capped with the compact thiocyanate ligand the Kagan group probed the photoconductivity of NC assemblies. **Fig. 21** depicts the photoconductivity for a CdSe NC thin film prepared by dropcasting from a dispersion of thiocyanate capped CdSe NCs. Scaled for device geometry and laser illumination, the currents recorded are 3 orders of magnitude larger than literature precedents prepared by dropcasting CdSe NCs and treating with n-butylamine (a relatively short ligand compared to that used in synthesis). The thiocyanate capped CdSe NC thin film photoconductive gain (I_{photo}/I_{dark}) is 10^3 at 10V and rises to 10^4 at 100V, equal to or better than that for n-butyl amine capped CdSe NC films.[56] The spectral response for

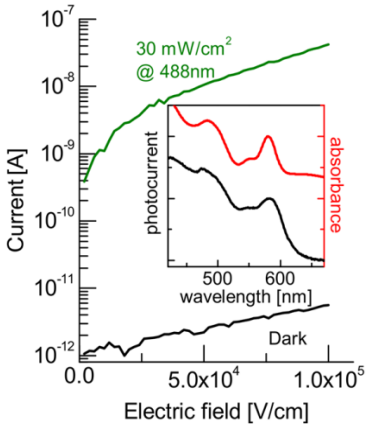

Fig. 21 Photoconductivity of thiocyanate capped CdSe NCs dropcast from DMF at 50 °C to form a NC film. Channel length is 10 µm and width is 150 µm. 30 mW/cm^2 illumination at 488 nm. (inset) Spectral response (black) for a similar film in comparison to the absorbance (red) of a film of the same material.

CdSe-SCN films, collected at a 1V bias (albeit limited by instrument bandpass), closes traces the optical absorption spectrum of the same NC film, collected away from the electrodes, reflecting the discrete, electronic structure characteristic of the quantum confined NC building blocks. This work was published in the work in the Journal of the American Chemical Society **133**, 15753 (2011).

Modulated Photoconductivities in Periodically Structured Nanocrystal Superlattices **-** The liquid-gas interface assembly process developed by Murray allowed the controlled assembly of NC superlattices varying periodically in NC thickness, presenting an exciting opportunity to structure NC films on multiple length scales and design corrugated, large-area heterojunctions for solar energy conversion. The Kagan group employed spatially resolved photoconductivity to map the photoconductivity in these striped PbSe NC films, assembled and then treated with hydrazine to increase the film conductivity. **Fig. 22(a)** shows an optical micrograph of a striped and treated NC membrane oriented to span Au electrodes. Overlaid on the micrograph of the sample, collected at high resolution, is a two-dimensional map of the local photoconductivity measured across the variation in NC film thickness. The oscillatory variation in photoconductivity, highlighted by a line-cut of the two-dimensional map **Fig. 22(b)**, reflects the variation in NC thickness in the membrane, with higher photoconductivity at the ridges compared to the troughs of the membrane. This work was also published in Nano Letters **11**, 841 (2011).

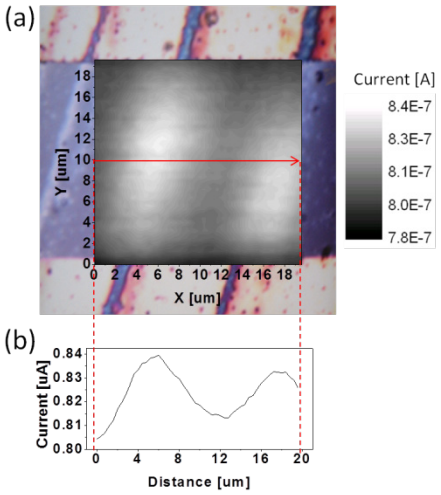

Fig. 22 (a) Optical micrograph of a striped PbSe NC membrane and local photoconductivity map and (b) line-cut of photoconductivity. Photoconductivity was collected using 488 nm excitation, with 10V applied across the junction.

7. Charge Transport in Nanocrystal Solids

Taking advantage of compact ligand exchange and doping [**sections 2** and **4**] to realize high mobility, II-VI and IV-VI NC thin films, we studied the mechanisms of charge injection and charge transport in two- and three-terminal device structures using temperature-dependent resistance and magnetoresistance measurements.

Charge Injection and Charge Transport in Nanocrystal Devices – In IV-VI semiconductor NCs there have been few studies separating charge injection from charge transport since high mobility, high conductivity materials have only recently been achieved and the barriers to injection are not as evident in these narrow bandgap materials. Kagan and Murray studied charge injection and transport in PbSe NC thin films by engineering the NC ligand exchange chemistry and surface passivation and the metallurgy of the contacts used in measurement.[14] **Fig. 23a** depicts 1) the small-organic and compact inorganic ligands selected to exemplify the range of chemistries introduced by us and the community, and 2) the metals chosen that are commonly used in NC devices and span a wide range of workfunctions (~4.2-5.5 eV).

In room temperature FET measurements [**Fig. 23b,c**], the small-organic ligand exchanged PbSe NC thin films showed low-current levels and highly hysteretic ambipolar characteristics, independent of the contact material, suggesting low mobility charge transport limits the device current levels. The compact inorganic ligand exchanged films showed significantly higher current levels that ranged from ambipolar to n-type and to p-type depending on the ligand chemistry and the metal workfunction. NC thin films exchanged with halides show greater electron currents and those exchanged with hydroxide had higher

hole currents, consistent with literature reports.[20] However for all the inorganic ligands, lower workfunction contacts gave high (lower) electron (hole) currents consistent with injection limited current, and in combination with low temperature measurements, indicate partial Fermi-level pinning at the metal-semiconductor NC interface (consistent with reports on PbSe NC photovoltaics[57]).

Thiocyanate-exchanged PbSe NCs were treated with $PbCl_2$ [as described in **section 4**].[11] The metal halide repairs metal vacancies and passivates the surface dramatically [**Fig. 23d**] increasing (x100) the room temperature electron mobility, compared to thiocyanate exchange only. The compact ligand exchange chemistries, such as thiocyanate, form locally, cubic ordered NCs [**inset Fig. 23a**]. Temperature-dependent electrical measurements show an insulator-metal transition from low mobility, low conductivity and thermally activated, nearest neighbor transport expected for small-organic ligand exchanged NC thin films to high mobility, high conductivity band-like transport for compact inorganic ligand exchanged NC thin films and for higher electron concentrations introduced by doping, passivation, and injection [**Fig. 23e**]. With the introduction of strongly coupled, high mobility, high conductivity NC thin films, charge injection and charge transport are important in materials and device design. This work was published in Nano Letters **14**, 6210 (2014).[14]

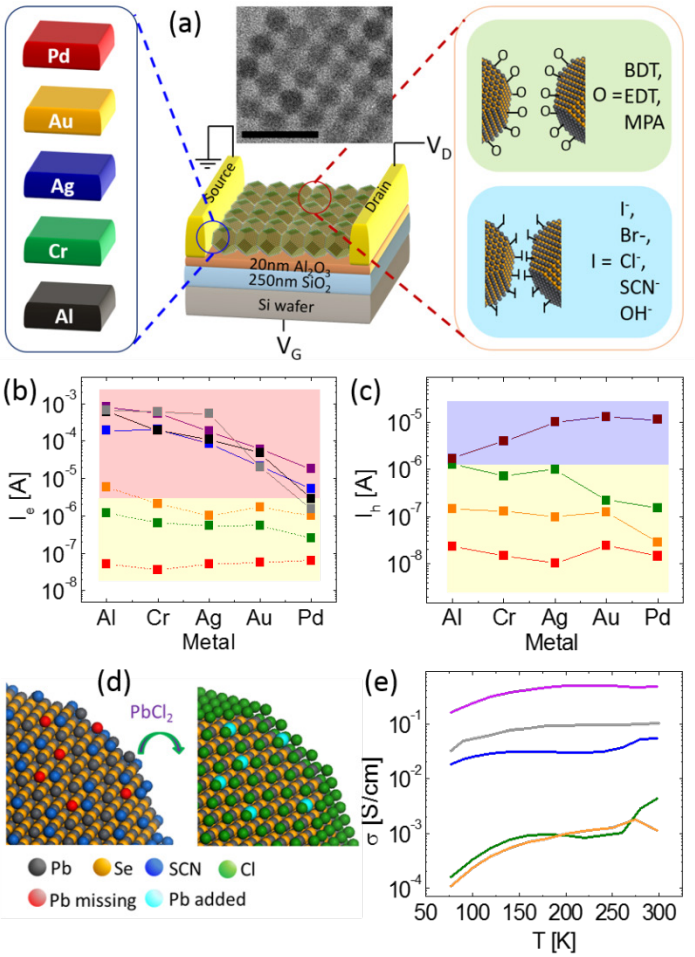

Fig. 23 (a) Schematic of PbSe NC thin films exchanged with small-organic and compact inorganic ligands forming the channel of FETs with different metal source-drain contacts. Inset middle, TEM image of thiocyanate and $PbCl_2$ treated NC thin films. (b) Electron and (c) hole currents at V_G=±50 V and V_{DS}=±50 V (+ for electrons/-for hole currents) for PbSe NC FETs with different metal contacts and treated with (red) benzenedithiol, (green) mercaptopropionic acid, (orange) ethanedithiol, (blue) tetrabutylammonium iodide, (purple) tetrabutylammonium bromide, (black) ammonium chloride, (gray) thiocyanate, and (brown) tetramethylammonium hydroxide. (d) Schematic of thiocyanate-treated PbSe NC surface before and after $PbCl_2$ treatment and (f) temperature-dependent electron conductivity calculated from Al-contact, FETs operating in the saturation regime with PbSe NC thin film channels treated with (green) mercaptopropionic acid, (orange) ethanedithiol, (blue) tetrabutylammonium iodide, (gray) thiocyanate, and (magenta) thiocyanate followed by $PbCl_2$ treatment.

Gate Induced Carrier Delocalization in Nanocrystal Field Effect Transistors - Kikkawa, Kagan and Murray used a combination of temperature dependent transport and magnetoresistance to demonstrate gate controlled carrier delocalization in indium-doped CdSe NC field effect transistors.[58] We found that using the gate to accumulate electrons in the NC channel increases the ``localization product'' (localization length times dielectric constant) describing transport at the Fermi level, as expected for Fermi level

changes near a mobility edge. Our measurements indicate that the localization length increases to significantly greater than the NC diameter.

Prior studies on these systems gave evidence for band-like transport near room temperature.[32] Here, our objective was to gain further insight into the spectrum of delocalized and localized states. Studying the system at much lower temperatures allows localized states to dominate conduction and to be probed with exponential sensitivity. **Fig. 24a** shows variable range hopping (VRH) behavior used to infer delocalization. These measurements, which were done with great care to ensure that voltage activation did not artificially suppress the VRH exponent, found an exponent of 2/3, in agreement with recent theories based on Coulomb Gap plus Gaussian broadening of localized states.[59] The inferred localization product (κa, where κ is the dielectric constant and a is the localization length) increases from 70 to 160 over the range of voltages shown. For any reasonable assumptions of dielectric constant, the data imply that transport involves states that are extended across many NCs [**Fig. 24b**].

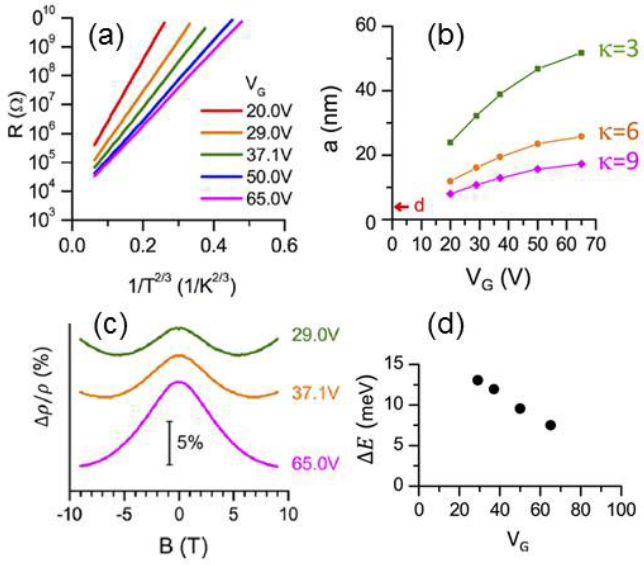

Fig. 24 Transport studies of a nanocrystal FET device. (a) Variable range hopping behavior with a 2/3 exponent is observed for a range of gate voltages. (b) Increases in localization distance with gate voltage for different assumed dielectric constants. (c) Changes in MR with gate bias at 7.5 K. (d) Change in inferred mobility gap with gate bias.

This result is predicted by and further supports the model used by Kagan and Murray to explain previously published higher temperature mobility data.[32] In particular, the positive gate voltage *decreases* the energetic mobility gap in the system, which results in reciprocal *increases* in localization length. Such effects have magnetic counterparts whose presence has also been verified. Specifically, the application of magnetic field also modulates the mobility gap and thus the localization length for ↑ and ↓ electron spin states. The resulting magnetoresistance effect [**Fig. 24c**] can be used to infer changes in the mobility gap [**Fig. 24d**]. Our data suggest that it may be possible to decrease the mobility gap in indium doped CdSe NC solids to zero, thereby achieving metallic conduction in this system. This work was published in Nano Letters, **14**, 5948 (2014).[4]

Flash-Photolysis, Time-Resolved Microwave Conductivity – The Kagan group constructed an apparatus for flash-photolysis, time-resolved microwave conductivity (FP-TRMC) measurements. The FP-TRMC measurement has proven to be an important tool for our exploration of the intrinsic conductivity of NC assemblies, complementing our device transport measurements**.** FP-TRMC provides a contactless probe of the zero-field, local carrier mobility and carrier lifetime, avoiding any complexities introduced by charge injection through metal-semiconductor junctions or disorder and defects on the 10-100 μm length scale in the channel of FETs.

We used FP-TRMC to probe the carrier mobility and lifetime in PbSe NC thin films treated with solutions of the metal salts of Na_2Se and $PbCl_2$. As described in **section 4**, the metal salt treatments tuned the Pb:Se stoichiometry and swept the Fermi energy throughout the NC thin film bandgap [**Fig. 25**]. A stoichiometric imbalance favoring excess Se heavily p-doped the NC thin film, shifted the Fermi energy toward the valence band, and yielded the highest TRMC mobility and lifetime. Introducing Pb first compensated the p-doping and shifted the Fermi level through mid-gap, decreasing the TRMC mobility. Further Pb addition created an excess of Pb, n-doped the NC thin film, moved the Fermi level to near the conduction band, and again increased the TRMC mobility. The increase in TRMC mobility as the Fermi energy was shifted toward the band edges by non-stoichiometry is consistent with the trend found in FET measurements and with the NC thin film density of states. This work was published in Chemical Physics **471**, 81 (2016).[60]

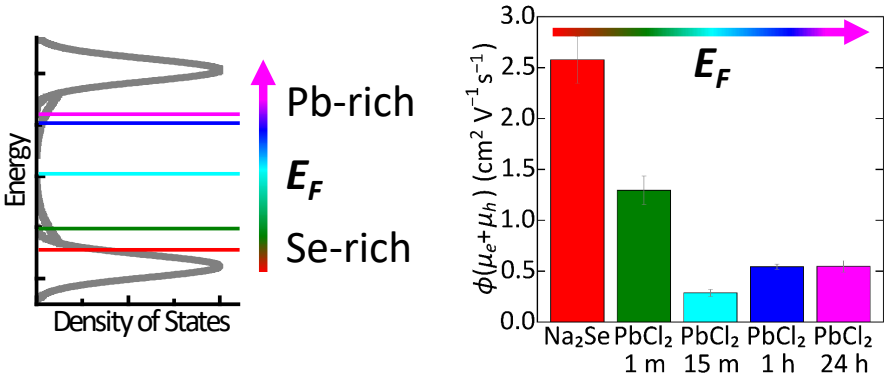

Fig. 25 (a) Schematic of the NC thin film density of states, marking the estimated positions of the Fermi energy as a function of the Pb:Se ratio in metal salt-treated PbSe NC thin films that were probed in FETs and by FP-TRMC. (b) The product of the quantum yield for charge generation and the sum of the electron and hole mobilities, ΦΣμ, at the lowest photoexcitation density in PbSe NC thin films treated with Na_2Se (red), Na_2Se followed by $PbCl_2$ for 1 min (green), 15 min (cyan), 1 h (blue), and 24 h (pink).

In combination with FET measurements, we have also used FP-TRMC to study the influence of indium doping on the dark mobility and the photogenerated mobility and lifetime in annealed, thiocyanate-exchanged CdSe NC thin films, mimicking the conditions used to fabricate high mobility FETs. In particular, while previous reports[11,32] have shown that increased surface trap passivation and doping increases the carrier mobility in NC thin films by introducing more carriers in higher energy, higher densities of states, studies are lacking that directly relate the effects of trap passivation and doping on carrier lifetime.[61] Yet, passivating surface defects and controlling the carrier concentration and mobility in NC thin films is prerequisite to designing electronic and optoelectronic devices. To carry out this investigation, we evaporate indium films ranging from 1 nm to 11 nm in thickness on top of approximately 40 nm thick, thiocyanate-capped, CdSe QD thin films and anneal the QD films at 300 °C to densify and drive diffusion

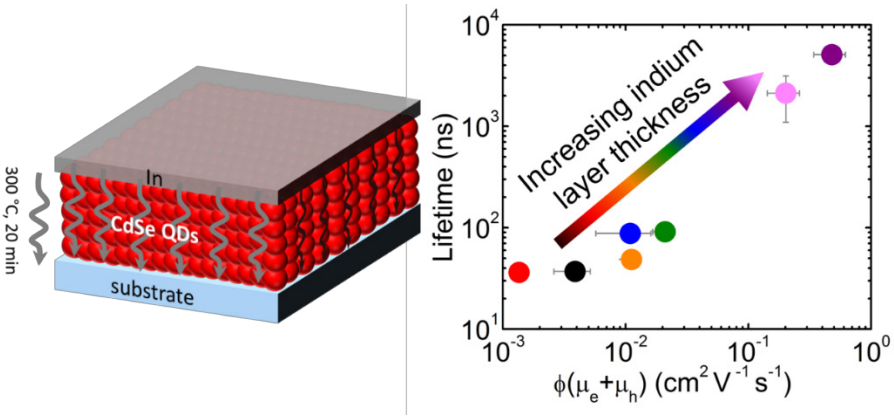

Fig. 26 (a) Schematic of CdSe NC thin film samples passivated and doped by evaporation and thermally-driven diffusion of indium. (b) Relationship between FP-TRMC carrier lifetime and the product of the quantum yield for charge generation and the sum of the electron and hole mobilities, ΦΣμ, as a function of indium concentration.

of indium through the films and probe the films in FETs and by FP-TRMC [**Fig. 26**]. As the amount of indium increases, the FET and FP-TRMC mobilities and the FP-TRMC lifetime increase. The increase in mobility and lifetime is consistent with increased indium passivating mid-gap and band-tail trap states and doping the films, shifting the Fermi energy closer to and into the conduction band. This work was published in J. Phys. Chem Lett, **6**, 4605 (2015).[62]

We have also applied the FP-TRMC measurement apparatus in collaboration with colleagues at Columbia University to study carrier diffusion lengths in single crystals of the three-dimensional organic-inorganic metal halide perovskites, receiving extraordinary attention for next-generation solar photovoltaic devices. This work was published in J. Phys. Chem. Lett, **7**, 3510 (2016) and in Nano Letters 17, 1727-1732 (2017).[63,64]

8. Nanocrystal Integrated Circuits

In phase one of the grant, we demonstrated the first example of NC electronic circuitry by constructing inverters, the simplest two-FET circuit.[65] In this example, the two NC FETs were externally wired together forming "discrete" electronics. In the last phase of the program, we developed processes to interconnect device layers on-chip enabling the demonstration of more complex analog and digital NC integrated circuits.

Low-voltage, Flexible CdSe NC Integrated Circuits (NMOS) – Building on our previous work achieving high mobility, CdSe NC FETs through a combination of exchange with the compact and non-corrosive ligand thiocyanate and doping by indium diffusion,[21,66] we reported the first NC integrated circuits.[5] Since CdSe NC FETs are n-type, we designed and fabricated inverters in a saturated load design, and developed processes for vertical interconnect access (VIA) holes to wire together device layers on-chip. We demonstrated low-voltage NC integrated inverters, amplifiers [**Fig. 27**] and ring oscillators, showing the promise of NCs as a class of materials for low-cost analog and digital circuitry. Taking advantage of the non-corrosive chemistry and uniform deposition of NC thin films, we fabricated these integrated circuits over large areas on flexible plastics. This work was published in Nature Communications **3:**1216 (2012).[5]

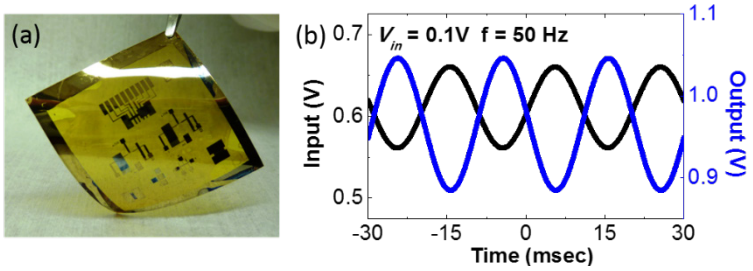

Fig. 27 (a) Photograph of NC integrated inverter and (b) operation as a voltage amplifier, characterized by its output waveform (blue, right axis) in response to a 50 Hz, 100 mV sinusoidal input on a 0.6 V DC bias (black, left axis).

PbSe NC Integrated Circuits (CMOS) – Thiocyanate-treated PbSe NC thin films, unlike n-type halide-treated or p-type hydroxyl-treated NC thin films, could be switched from unipolar, n-type to unipolar, p-type by engineering the metallurgy of the contacts used to construct devices [**Fig. 28a**]. We took advantage of metal contact engineering to build the first integrated CMOS NC inverters.[14]

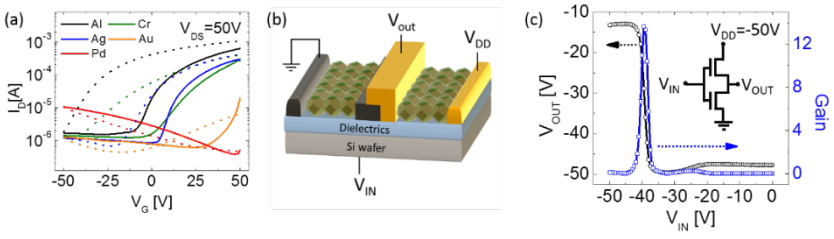

Fig. 28 (a) Transfer characteristics of thiocyanate-exchanged PbSe NC thin film FETs with different metal contacts. (b) Schematic and (c) transfer characteristics of an integrated complementary metal oxide semiconductor (CMOS) inverter constructed from an n-type thiocyanate-exchanged PbSe NC FET with Al contacts and a p-type thiocyanate-exchanged PbSe NC FET with Au contacts.

Note CMOS borrows its name from complementary metal oxide semiconductor silicon FETs, in which a combination of n-type and p-type FETs are used to fabricate lower power, lower noise, and higher gain/speed circuitry. Here by using a single thiocyanate-exchanged PbSe NC thin film, we could deposit and connect different metal layers [**Fig. 28b**] to demonstrate integrated CMOS NC circuitry [**Fig. 28c**]. This work was published in Nano Lett. **14**, 6210 (2014).[14]

9. PLASMONIC NCS

In the first few years of the program, we explored plasmonic NCs as a third building block in NC superlattices. We developed synthetic methods to broaden the available plasmonic NC materials and investigated compact ligand exchange methods, as were also used for semiconductor NCs, to design their electrical conductivity and plasmonic response.

Synthesis of heavily-doped, wide band-gap plasmonic, semiconductor nanocrystals - Heavily-doped wide band-gap semiconductor NCs are excellent candidates for solution-cast transparent electrodes in photovoltaics or other optoelectronic devices and as plasmonic NC building blocks. We developed a generalized method to synthesize doped oxides with aliovalent cations by thermal decomposition of metal carboxylates at elevated temperature.[67] The synthesis allows controlled doping of the NCs with free electron concentrations of 10^{19}-10^{21} cm^{-3}. In a dispersed state, these materials demonstrate a localized surface plasmon resonance tunable in the mid- and near-infrared related to the free carrier concentration (*i.e.* doping level) [**Fig. 24**]. When condensed into solids, they can be annealed to make transparent and highly-conductive films with conductivities as high as 200 S/cm. We demonstrated the use of these NCs as inks for the transparent window of a quantum dot sensitized photovoltaic cells. This work was published in Chemistry of Materials **26**, 4579 (2014).

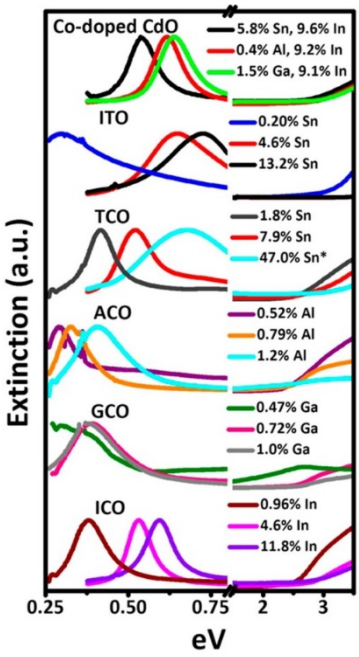

Fig. 24 Ultraviolet, visible and infrared extinction spectra of doped-oxide NCs dispersed in tetrachloroethylene. Each grouping represents three samples of the doped oxide NCs, except for the top grouping, which shows the extinction spectra of codoped Al- and In-doped CdO, Ga- and In-doped CdO, and Sn- and In-doped CdO. The starred samples indicates a distinct phase $CdSnO_3$.

Ligand Exchange of Plasmonic Au or Ag NCs to Design their Electrical Properties and Plasmonic Response - In the first phase of the program, we had preliminary evidence to show that the compact ligand thiocyanate could also be employed to exchange the ligands on the surface of plasmonic Au and Ag NCs. Here we have shown that we can transform electrically and optically insulating Au and Ag NC thin films, deposited from colloidal solutions, into highly conductive optical and electronic materials.[68,69] Structural, analytical, optical and electrical measurements were used to follow the transformation. The insulator to metal transition gives rise to a 10^{10} increase in DC conductivity, within a factor of 5 and 10 of thermally evaporated Ag and Au films, respectively, and a dielectric permittivity that is altered from everywhere positive (insulator) to everywhere negative (Drude metal) throughout the visible-to-NIR.

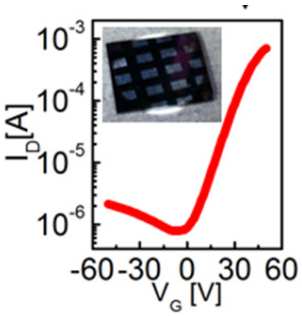

Fig. 25 Transfer characteristics of a Pb-enriched PbSe NC FET with Ag NC source and drain electrodes. (Inset) Photograph of FET.

We used imprint- and photo- lithographies to pattern Au and Ag thin films. By patterning Ag NC thin films and using thiocyanate exchange, we fabricated conductive electrodes. We combined these Ag NC-based

electrodes with thiocyanate-exchanged and Pb-enriched PbSe NC thin films to form NC FETs with high electron mobilities of 5 cm^2/Vs [**Fig. 25**] and thiocyanate-exchanged, indium doped CdSe NC to form all-NC FETs. This work was published in Nano Letters **13**, 350 (2013) and ACS Nano **8**, 2746 (2014).

10. BROAD IMPACT ON THE SCIENTIFIC COMMUNITY: Many of the scientific accomplishments of this work were highlighted in two invited review papers written by PIs Kagan and Murray on "Charge Transport in Strongly Coupled Nanocrystal Solids," Nat. Nano **10**, 1013-1026 (2015) and on "Building devices from colloidal quantum dots," Science 6302, aac5523-1 (2016).

11. SUMMARY OF SUPPORTED PUBLICATIONS AND ACKNOWLEDGEMENTS OF AWARD NO. DESC0002158

Primary Support from DOE-BES Materials Chemistry Program:

A1. X. C. Ye, J. E. Collins, Y. J. Kang, J. Chen, D. T. N. Chen, A. G. Yodh, and C. B. Murray, "Morphologically controlled synthesis of colloidal upconversion nanophosphors and their shape-directed self-assembly," *Proceedings of the Natural Academy of Sciences* **107**, 22430-22435 (2010).

"X.Y. acknowledges primary support from the Department of Energy Basic Energy Science division through award DE-SC0002158 while C.B.M. received partial support for his supervisor role from the Department of Energy Basic Energy Science division through award DE-SC0002158…"

A2. D.-K. Ko, J. J. Urban, C. B. Murray, ""Carrier Distribution and Dynamics of Nanocrystal Solids Doped with Artificial Atoms" *Nano Letters* **10**, 1842-1847 (2010).

"This work was supported in part by the U.S. Department of Energy, Office of Basic Energy Sciences, Division of Materials Sciences and Engineering under Award # DE-SC0002158 (C.B.M. and D.-K.K.) enabling the X-ray scattering studies, structural characterization, and analysis of all experimental results."

A3. X.Ye, Chen, J. Chen, C. B. Murray, "Polymorphism in Self-Assembled AB(6) Binary Nanocrystal Superlattices" *Journal of the American Chemical Society* **133**, 2613-2620 (2011).

"We acknowledge financial support from the Department of Energy Basic Energy Science division through award DE-SC0002158 for synthesis of plasmonic NCs and assembly and characterization of BNSLs (X.Y.)"

A4. Y.-W. Liu, D.-K. Ko, S. J. Oh, T. R. Gordon, V. Doan-Nguyen, T. Paik, Y. Kang, X. Ye, L. Jin, C. R. Kagan, and C. B. Murray, "Near-Infrared Absorption of Monodisperse Silver Telluride (Ag_2Te) Nanocrystals and Photoconductive Response of Their Self-Assembled Superlattices," *Chemistry of Materials* **23**, 4657-4659, (2011).

"Y.-W.L. and S.J.O.'s respective roles in Ag_2Te synthesis and photoconductive studies were supported by the U.S. Department of Energy, Office of Basic Energy Sciences, Division of Materials Sciences and Engineering (Award DE-SC0002158) as were CBM and C.R.K.'s supervisory roles."

A5. S. J. Oh, D. K. Kim, C. R. Kagan, "Remote Doping and Schottky Barrier Formation in Strongly Quantum Confined Single PbSe Nanowire Field-Effect Transistors," *ACS Nano* **6**, 4328-4334 (2012).

"S.J.O. and C.R.K. acknowledge support by the U.S. Department of Energy, Office of Basic Energy Sciences, Division of Materials Sciences and Engineering (Award DE-SC0002158)…"

A6. S. J. Oh, N. E. Berry, J.-H. Choi, E. A. Gaulding, T. Paik, S.-H. Hong, C. B. Murray, C. R. Kagan. Stoichiometric Control of Lead Chalcogenide Nanocrystal Solids to Enhance Their Electronic and Optoelectronic Device Performance. *ACS Nano* **7** 2413-2421 (2013).

"The synthesis of PbS and PbSe nanocrystals and the fabrication and characterization of bottomcontact field-effect transistors used to study the diffusion length of lead and selenium, devices for Hall-effect measurements, and Schottky barrier solar cells were supported by the U.S. Department of Energy Office of Basic Energy Sciences, Division of Materials Science and Engineering, under Award No. DESC0002158."

A7. D.C. Reifsnyder, X. Ye, T.R. Gordon, C. Song, C.B. Murray. Three-Dimensional Self-Assembly of Chalcopyrite Copper Indium Diselenide Nanocrystals into Oriented Films. *ACS Nano* **7**, 4307-4315 (2013).

"D.C.R. and C.B.M. acknowledge support from the U.S. Department of Energy Office of Basic Energy Sciences, Division of Materials Science and Engineering (Award No. DE-SC0002158)."

A8. B.T. Diroll, A. Koschitzky, C.B. Murray. Tunable Optical Anisotropy in Seeded CdSe/CdS Nanorods. *J. Phys. Chem. Lett.* **5**, 85-91 (2014).

"B.T.D., A.K., and C.B.M. acknowledge support from DOE Office of Basic Sciences under award No. DE-SC0002158."

A9. B.T. Diroll, C.B. Murray. High Temperature Photoluminescence of CdSe/CdS Core/Shell Nanoheterostructures. *ACS Nano* **8**, 6466-6474 (2014).

"This work was supported by the DOE, Office of Basic Energy Sciences, Division of Materials Science Award No. De-SC0002158."

A10. S. J. Oh, N. E. Berry, J.-H. Choi, E. A. Gaulding, H. Lin, T. Paik, B. T. Diroll, S. Muramoto, C. B. Murray, C. R. Kagan. Designing High-Performance PbS and PbSe Nanocrystal Electronic Devices through Stepwise, Post-Synthesis, Colloidal Atomic Layer Deposition. *Nano Lett.* **14**, 1559-1566 (2014).

"The lead chalcogenide NC synthesis, small and wide-angle x-ray scattering, sample preparation for all structural, optical, and electrical measurements, absorption spectroscopy, EDX measurements, Hall measurements, and FET characterization are supported by the U.S. Department of Energy Office of Basic Energy Sciences, Division of Materials Science and Engineering, under Award No. DE-SC0002158."

A11. B.T. Diroll, T.R. Gordon, E.A. Gaulding, D.K. Klein, T. Paik, H.J. Yun, E.D. Goodwin, D. Damodhar, C.R. Kagan, C.B. Murray. Synthesis of N-Type Plasmonic Oxide Nanocrystals and the Optical and Electrical Characterization of their Transparent Conducting Films. *Chemistry of Materials* **26**, 4579-4588 (2014).

"Primary support for work on thin film optical, structural, and electronic properties came from the DOE Office of Basic Energy Sciences, Division of Materials Science Award no. DE-SC0002158."

A12. M. E. Turk, J.-H. Choi, S. J. Oh, A. T. Fafarman, B. T. Diroll, C. B. Murray, C. R. Kagan, J. M. Kikkawa, Gate Induced Carrier Delocalization in Quantum Dot (QD) Field-Effect Transistors (FETs). *Nano Lett.* **14**, 5948-5952 (2014).

"All aspects of this work supported by the U.S. Department of Energy Office of Basic Energy Sciences, Division of Materials Science and Engineering, under Award No. DE-SC0002158."

A13. B.T. Diroll, V.V.T. Doan-Nguyen, M. Cargnello, E.A. Gaulding, C.R. Kagan, C.B. Murray. X-ray Mapping of Nanoparticle Superlattice Thin Films. *ACS Nano* **8** (12), 12843-12850 (2014).

"Sample preparation and microscopy was supported by the Department of Energy, Office of Basic Energy Sciences, Division of Materials Science Award No. De-SC0002158."

A14. S. J. Oh, Z. Wang, N. E. Berry, J.-H. Choi, T. Zhao, E. A. Gaulding, T. Paik, Y. Lai, C. B. Murray, C. R. Kagan. Engineering Charge Injection and Charge Transport for High Performance Nanocrystal Thin Film Devices and Circuits. *Nano Lett.* **14**, 6210-6216 (2014).

"We thank the U.S. Department of Energy Office of Basic Energy Sciences, Division of Materials Science and Engineering, under Award No. DE-SC0002158 for primary support of this work for NC synthesis, NC thin-film deposition, NC device fabrication, engineering of contact metallurgy and ligand exchange chemistry, FTIR and EDX spectroscopies, room and temperature-dependent transistor and conductivity measurements, circuit characterization, and data analysis."

A15. M. V. Kovalenko, L. Manna, A. Cabot, Z. Hens, D. V. Talapin, C. R. Kagan, V. I. Klimov, A. L. Rogach, P. Reiss, D. J. Milliron, P. Guyot-Sionnest, G. Konstantatos, W. J. Parak, T. Hyeon, B. A. Korgel, C. B. Murray, W. Heiss, Prospects of Nanoscience with Nanocrystals. *ACS Nano*, invited Focus, **9**, 1012-1057 (2015).

"C.R.K. and C.B.M. acknowledge financial support from the U.S. Department of Energy Office of Basic Energy Sciences, Division of Materials Science and Engineering (Award No. DE-SC0002158)."

A16. M. E. Turk, P. M. Vora, A. T. Fafarman, B. T. Diroll, C. B. Murray, C. R. Kagan, J. M. Kikkawa. Ultrafast Electron Trapping in Ligand-Exchanged Quantum Dot Assemblies. *ACS Nano* **9**, 1440-1447 (2015).

"All aspects of this work are supported by the U.S. Department of Energy Office of Basic Energy Sciences, Division of Materials Science and Engineering, under Award No. DE-SC0002158."

A17. E. A. Gaulding, B. T. Diroll, E. D. Goodwin, Z. J. Vrtis, C. R. Kagan, C. B. Murray. Deposition of Wafer-Scale Single Component and Binary Nanocrystal Superlattice Thin Films *Via* Dip-coating. *Adv. Mater*. **27**, 2846-2851 (2015).

"Primary support of this research, including development of the dip-coating process, was from the U.S. Department of Energy Office of Basic Energy Sciences, Division of Materials Science and Engineering, under Award No. DE-SC0002158."

A18. B.T. Diroll, N.J. Greybush, C.R. Kagan, C.B. Murray. Smectic Nanorod Superlattices Assembled on Liquid Subphases: Structure, Orientation, Defects, and Optical Polarization. *Chem. Mater.* **27**, 2998-3008 (2015).

"Primary support for this work comes from the Department of Energy, Office of Basic Energy Sciences, Division of 705 Materials Science, Award No. De-SC0002158,"

A19. C. R. Kagan, C. B. Murray. Charge Transport in Strongly-Coupled Quantum Dot Solids. *Nat. Nano*, **10**, 1013-1026 (2015).

"The authors acknowledge the US Department of Energy Office of Basic Energy Sciences, Division of Materials Science and Engineering, under Award No. DE-SC0002158, for primary support of this manuscript."

A20. E. D. Goodwin, D. B. Straus, E. A. Gaulding, C. B. Murray, C. R. Kagan, The effects of inorganic surface treatments on photogenerated carrier mobility and lifetime in PbSe quantum dot thin films, *Chem. Phys.* **471**, 81-88 (2016).

"We thank the U.S. Department of Energy Office of Basic Energy Sciences, Division of Materials Science and Engineering, under Award No. DE-SC0002158 for primary support of this work."

A21. B. T. Diroll, E. A. Gaulding, C. R. Kagan, C. B. Murray, Spectrally-Resolved Dielectric Functions of Solution-Cast Quantum Dot Thin Films, Chem Mater, **27**, 6463-6469 (2015).

"This work was supported by the Department of Energy, Office of Basic Sciences, Division of Materials Science, Award No. DESC0002158."

A22. D. B. Straus, E. D. Goodwin, E. A. Gaulding, S. Muramoto, C. B. Murray, C. R. Kagan, Increased Carrier Mobility and Lifetime in CdSe Quantum Dot Thin Films through Surface Trap Passivation and Doping, *J. Phys. Chem. Lett*, **6**, 4605-4609 (2015).

"We thank the U.S. Department of Energy Office of Basic Energy Sciences, Division of Materials Science and Engineering, under Award No. DE-SC0002158 for primary support of this work."

A23. C. R. Kagan, E. Lifshitz, E. H. Sargent, D. V. Talapin, Building devices from colloidal quantum dots, *Science* **6302**, aac5523-1 (2016).

"C.R.K. gratefully acknowledges the U.S. Department of Energy, Office of Basic Energy Sciences, Division of Materials Science and Engineering, under award DE-SC0002158 for support."

A24. S. J. Oh, D. B. Straus, T. Zhao, J.-H. Choi, S.-W. Lee, E. A. Gaulding, C. B. Murray, C. R. Kagan, Engineering the surface chemistry of lead chalcogenide nanocrystal solids to enhance carrier mobility and lifetime in optoelectronic devices, *Chem, Commun.* 53, 728-731 (2017).

"The work is primarily supported by the U.S. Department of Energy Office of Basic Energy Sciences, Division of Materials Science and Engineering, under Award DE-SC0002158 for NC synthesis and for the fabrication, measurement, and chemical, electronic and optoelectronic analysis of NC thin films and their FETs, photoconductors, and solar cells."

A25. X. Ye, J. Chen, M. EIrrgang, M. Engel, A. Dong, S. C. Glotzer, and C. B. Murray, "Quasicrystalline nanocrystal superlattice with partial matching rules", *Nature Materials* **16**, 214-220 (2017).

"X.Y. and C.B.M. were supported by the US Department of Energy Office of Basic Energy Sciences, Division of Materials Science and Engineering under Award No. DE-SC0002158."

A26. B. T. Diroll, N. Gogotsi, and C. B. Murray, "Statistical Description of CdSe/CdS Dot-in-Rod Heterostructures Using Scanning Transmission Electron Microscopy", *Chem. Mater.*, **28** (10), 3345–3351 (2016).

"This work was supported by the Department of Energy, Office of Basic Sciences, Division of Materials Science, Award No. DE-SC0002158."

50% Support from DOE-BES Materials Chemistry Program:

B1. D. K. Kim*, Y. Lai*, B. T. Diroll, C. B. Murray, C. R. Kagan, Flexible and low-voltage integrated circuits constructed from high-performance nanocrystal transistors, *Nat. Comm.* **3:**1216 (2012).

"The fabrication, characterization and analysis of flexible NC integrated circuits (inverters, amplifiers and ring oscillators) was supported by the U.S. Department of Energy Office of Basic Energy Sciences, Division of Materials Science and Engineering, under award number DE-SC0002158."

Secondary Support from DOE-BES Materials Chemistry:

C1. J. Chen, A. G. Dong, J. Cai, X. C. Ye, Y. J. Kang, J. K. Kikkawa, C. B. Murray, "Collective Dipolar Interactions in Self-Assembled Magnetic Binary Nanocrystal Superlattice Membranes", *Nano Letters* **10**, 5103-5108 (2010).

"X.Y. acknowledges support from the Department of Energy Basic Energy Science division under award number DE-SC0002158 for structural characterization."

C2. A. Dong, J. Chen, S. J. Oh, W.-K. Koh, F. Xiu, X. Ye, D.-K. Ko, K. L. Wang, C. R. Kagan, C. B. Murray, "Multiscale Periodic Assembly of Striped Nanocrystal Superlattice Films on a Liquid Surface," *Nano Letters* **11**, 841-846 (2011).

S.J.O., C.R.K., X.Y., and C.B.M. acknowledge support from the U.S. Department of Energy, Office of Basic Energy Sciences, Division of Materials Sciences and Engineering under Award No. DE-SC0002158.

C3. Y. J. Kang, X. C. Ye, C. M. Murray, "Size- and Shape-Selective Synthesis of Metal Nanocrystals and Nanowires Using CO as a Reducing Agent", *Angewandte Chemie-International Edition* **49**, 6156-6159 (2010).

"studies of plasmonic gold nanowires were funded by the Department of Energy's Division of Basic Energy Sciences through Award: DE-SC0002158 (X.Y. & C.B.M.).

C4. A. G. Dong, X. C. Ye, J. Chen, Y. J. Kang, T. G. Gordon, J. M. Kikkawa, Y. C. Ye, and C. B. Murray, "A Generalized Ligand-Exchange Strategy Enabling Sequential Surface Functionalization of Colloidal Nanocrystals" *Journal of the American Chemical Society* **133**, 998-1006 (2011).

"X.Y.'s contributions with $NaYF_4$nanophosphors were supported by the Department of Energy's Division of Basic Energy Sciences under award number DE-SC0002158…"

C5. A. Dong, X.C. Chen, J. Chen, and C. B. Murray, "Two-Dimensional Binary and Ternary Nanocrystal Superlattices: The Case of Monolayers and Bilayers", *Nano Letters* **11,** 1804-1809 (2011).

"X.Y. acknowledges support from the Department of Energy Basic Energy Science division through award DE-SC0002158 for development of $NaYF_4$ NCs…"

C6. Chang-Hee Cho, Carlos O. Aspetti, Michael E. Turk, James M. Kikkawa, Sung-Wook Nam, and Ritesh Agarwal, "Tailoring hot-excitonic emission in semiconducting nanowires via whispering gallery nanocavity plasmons", *Nature Materials* **10**, 669-675 (2011).

"Time-resolved photoluminescence work was supported by the Department of Energy BES under Award No. DESC0002158."

C7. A. T. Fafarman, W.-K. Koh, B. T. Diroll, D. K. Kim, D.-K. Ko, S. J. Oh, X. Ye, V. Doan-Nguyen, M. R. Crump, D. C. Reifsnyder, C. B. Murray, and C. R. Kagan, "Thiocyanate Capped Nanocrystal Colloids: A Vibrational Reporter of Surface Chemistry and a Solution-based Route to Enhanced Coupling in Nanocrystal Solids," *Journal of the American Chemical Society* **133**, 15753–15761, (2011).

"S.J.O. and D.C.R. acknowledge support from the U.S. Department of Energy Office of Basic Energy Sciences, Division of Materials Science and Engineering, under Award No. DE-SC0002158."

C8. W.-K. Koh , S. R. Saudari , A. T. Fafarman , C. R. Kagan , and C. B. Murray, "Thiocyanate-capped PbS nanocubes: ambipolar transport enables quantum dot-based circuits on a flexible substrate," *Nano Letters* **11**, 4764–4767 (2011).

"A.T.F. and C.R.K. acknowledge support from the U.S. Department of Energy Office of Basic Energy Sciences, Division of Materials Science and Engineering under Award No. DE-SC0002158."

C9. X. X. Ye, L. Jin, H. Caglayan, J. Chen, G. Xing, C. Zheng, V. Doan-Nguyen, Y. Kang, N. Engheta, C. R. Kagan, C. B. Murray,"Improved Size-Tunable Synthesis of Monodisperse Gold Nanorods through the Use of Aromatic Additives," *ACS Nano*, **6**, 2804-2817 (2012).

" G.X. and C.R.K. acknowledge support from the U.S. Department of Energy, Office of Basic Energy Sciences, Division of Materials Science and Engineering, under Award No. DE-SC0002158."

C10. J.-H. Choi, A.T. Fafarman, S. J. Oh, D.-K. Ko, D. K. Kim, B. T. Diroll, S. Muramoto, J. G. Gillen, C. B. Murray, C. R. Kagan, "Band-like transport in strongly-coupled and doped quantum dot solids: A route to high-performance thin-film electronics," *Nano Lett* **12**, 2631-2638 (2012).

"S.J.O. and C.R.K. acknowledge support from the U.S. Department of Energy Office of Basic Energy Sciences, Division of Materials Science and Engineering, under Award No. DE-SC0002158."

C11. M. Saboktakin, X. Ye, S. J. Oh, S.-H. Hong, A. T. Fafarman, U. K. Chettiar, N. Engheta, C. B. Murray, C. R. Kagan. Metal-Enhanced Upconversion Luminescence Tunable through Metal Nanoparticle-Nanophosphor Separation. *ACS Nano* **6**, 8758-8766 (2012).

"S.J.O., A.T.F., and C.R.K. acknowledge support from the U.S. Department of Energy, Office of Basic Energy Sciences, Division of Materials Science and Engineering, under Award No. DESC0002158."

C12. A. T. Fafarman, S.-H. Hong, H. Caglayan, X. Ye, B. T. Diroll, T. Paik, N. Engheta, C. B. Murray, C. R. Kagan. Chemically Tailored Dielectric-to-Metal Transition for the Design of Metamaterials from Nanoimprinted Colloidal Nanocrystals, *Nano Lett*. **13**, 350-357 (2013).

"The work on Au nanocrystal thin film deposition and ligand exchange, conductivity, and atomic force microscopy was supported by the U.S. Department of Energy Office of Basic Energy Sciences, Division of Materials Science and Engineering, under Award No. DE-SC0002158."

C13. J. Chen, X. Ye, S. J. Oh, J. M. Kikkawa, C. R. Kagan, C. B. Murray, Bistable Magnetoresistance Switching in Exchange-Coupled $CoFe_2O_4$-Fe_3O_4 Binary Nanocrystal Superlattices by Self-Assembly and Thermal Annealing. *ACS Nano* **7**, 1478-1486 (2013).

"S.J.O. and C.R.K. acknowledge U.S. Department of Energy Office of Basic Energy Sciences, Division of Materials Science and Engineering, under award No. DE-SC0002158."

C14. Y. Kang, X. Ye, J. Chen, L. Qi, R. E. Dias, V. Doan-Nguyen, G. Xing, C. R. Kagan, J. Li, R. J. Gorte, E. A. Stach, C. B. Murray. Engineering Catalytic contacts and Thermal Stability: Gold/Iron Oxide Binary Nanocrystal Superlattices for CO Oxidation**.** *J. Am. Chem. Soc.* **135**, 1499-1505 (2013).

"G.X. and C.R.K. acknowledge support from the U.S. Department of Energy, Office of Basic Energy Sciences, Division of Materials Science and Engineering, under Award No. DE-SC0002158."

C15. D. K. Kim, A. T. Fafarman, B. T. Diroll, S. H. Chan, T. R. Gordon, C. B. Murray, C. R. Kagan. Solution-Based Stoichiometric Control over Charge Transport in Nanocrystalline CdSe Devices. *ACS Nano* **7**, 8760-8770 (2013).

"The CdSe nanowire synthesis was supported by the U.S. Department of Energy Office of Basic Energy Sciences, Division of Materials Science and Engineering, under Award No. DE-SC0002158."

C16. X. Ye, Y. Gao, J. Chen, D.C. Reifsnyder, C. Zheng, C.B. Murray. Seeded Growth of Monodisperse Gold Nanorods using Bromide-Free Surfactant Mixtures. *Nano Lett.* **13**, 2163-2171 (2013).

"D.C.R. acknowledges supports from DOE Office of Basic Energy Sciences, Division of Materials Science and Engineering, under Award No. DE-SC0002158."

C17. B.T. Diroll, T. Dadosh, A. Koschitzky, Y.E. Goldman, C.B. Murray. Interpreting the Energy-Dependent Anisotropy of Colloidal Nanorods Using Ensemble and Single-Particle Spectroscopy. *J. Phys. Chem. C* **117**, 23928-23937 (2013).

"… DOE Office of Basic Sciences under Award DE-SC0002158 to support spectroscopy."

C18. X. Ye, J. Chen, M. Engel, J. A. Millan, W. Li, L. Qi, G. Xing, J. E. Collins, C. R. Kagan, J. Li, S. C. Glotzer, C. B. Murray. Competition of shape and interaction patchiness for self-assembling nanoplates. *Nature Chemistry,* **5**, 466-473 (2013).

"G.X. and C.R.K. acknowledge support from the US Department of Energy, Office of Basic Energy Sciences, Division of Materials Sciences and Engineering (Award DE-SC0002158)."

C19. J.-H. Choi, S. J. Oh, Y. Lai, D. K. Kim, T. Zhao, A. T. Fafarman, B. T. Diroll, C. B. Murray, C. R. Kagan. *In Situ* Repair of High-Performance, Flexible Nanocrystal Electronics for Large-Area Fabrication and Operation in Air. *ACS Nano* **7**, 8275-8283 (2013).

"The synthesis of CdSe NCs, the development of the ultrathin ALD oxide, the photolithographic patterning of FETs, and the fabrication and characterization of flexible FETs were supported by the U.S. Department of Energy Office of Basic Energy Sciences, Division of Materials Science and Engineering, under Award No. DE-SC0002158."

C20. X. Ye, J. Millan, M. Engel, J. Chen, B.T. Diroll, S. Glotzer, C.B. Murray. Shape Alloys of Nanorods and Nanospheres from Self-Assembly. *Nano Lett.* **13,** 4980-4988 (2013).

"B.T.D.'s work on the synthesis of semiconductor nanocrystals was supported in part by the U.S. Department of Energy Office of Basic Energy Sciences, Division of Materials Science and Engineering, under award No. DE-SC0002158."

C21. T. Paik, S.-H. Hong, E. A. Gaulding, H. Caglayan, T. R. Gordon, N. Engheta, C. R. Kagan, C. B. Murray. Solution-Processed Phase-Change VO_2 Metamaterials from Colloidal Vanadium Oxide (VO_x) Nanocrystals. *ACS Nano* **8**, 797-806 (2014).

"E.A.G.'s temperature-dependent electrical measurement of VO2 thin films was supported by the U.S. Department of Energy Office of Basic Energy Sciences, Division of Materials Science and Engineering Award No. DE-SC0002158."

C22. A. T. Fafarman, S.-H. Hong, S. J. Oh, H. Caglayan, X. Ye, B. T. Diroll, N. Engheta, C. B. Murray, C. R. Kagan. Air-Stable, Nanostructured Electronic and Plasmonic Materials from Solution-Processable, Silver Nanocrystal Building Blocks. *ACS Nano* **8**, 2746-2754 (2014).

"The work on silver nanocrystal thin film deposition and ligand exchange, conductivity, atomic force microscopy, and PbSe nanocrystal FET fabrication and characterization was supported by the U.S. Department of Energy Office of Basic Energy Sciences, Division of Materials Science and Engineering, under Award No. DE-SC0002158."

C23. X. Ye, D.R. Hickey, J. Fei, B.T. Diroll, T. Paik, J. Chen, C.B. Murray. Seeded Growth of Metal-Doped Plasmonic Oxide Heterodimer Nanocrystals and Their Chemical Transformation. *J. Am. Chem. Soc.* **136**, 5106-6115 (2014).

"D.R.H. and B.T.D. are grateful for support from the U.S. Department of Energy Office of Basic Energy Sciences, Division of Materials Science and Engineering, under award no. DE-SC0002158."

C24. X. Ye, J. Fei, B.T. Diroll, T. Paik, C.B. Murray. Expanding the Spectral Tunability of Plasmonic Resonances in Doped Metal-Oxide Nanocrsytals through Cooperative Cation-Anion Doping. *J. Am. Chem. Soc.* **136**, 11680-11686 (2014).

"Partial support from the U.S. Department of Energy Office of Basic Energy Sciences, Division of Materials Science and Engineering, under award no. DE-SC0002158 enabled the X-ray analysis including SAXS studies."

C25. V.V.T. Doan-Nguyen, S.A.J. Kimber, D. Pontoni, D.R. Hickey, B.T. Diroll, X. Yang, M. Miglierini, C.B. Murray, S.J.L. Billinge. Bulk-Metallic Glass-Like Signal in Small Metallic Nanoparticles. *ACS Nano* **8**, 6163-6170 (2014).

"SAXS and HRTEM data collection was supported from the DOE, Office of Science, Office of Basic Energy Sciences (BES), Division of Materials Science and Engineering, under Award Number DE-SC0002158."

C26. N. J. Greybush, M. Saboktakin, X. Ye, C. Della Giovampaola, S. J. Oh, N. E. Berry, N. Engheta, C. B. Murray, C. R. Kagan. Plasmon-Enhanced Upconversion Luminescence in Single Nanophosphor-Nanorod Heterodimers Formed through Template-Assisted Self-Assembly. *ACS Nano* **8**, 9482-9491 (2014).

"Construction of the PL mapping setup was supported by the U.S. Department of Energy Office of Basic Energy Sciences, Division of Materials Science and Engineering under Award No. DE-SC0002158."

C27. Y. Lai, H. Li, D. K. Kim, B. T. Diroll, C. B. Murray, C. R. Kagan, Low-Frequency (1/f) Noise in Nanocrystal Field-Effect Transistors. *ACS Nano* **8**, 9664-9672 (2014).

"We thank the U.S. Department of Energy Office of Basic Energy Sciences, Division of Materials Science and Engineering, under Award No. DE-SC0002158 for NC synthesis and EDX spectroscopy."

C28. M. Cargnello, B.T. Diroll, E.A. Gaulding, C.B. Murray. Enhanced Energy Transfer in Quasi-Quaternary Nanocrystal Superlattices. *Adv. Mat.* **26**, 2419-2423 (2014).

"B.T.D. and E.A.G. acknowledge support from the U.S. Department of Energy Office of Basic Energy Sciences, Division of Materials Science and Engineering, under Award No. DE-SC0002158."

C29. E. D. Goodwin, B. T. Diroll, S. J. Oh, T. Paik, C. B. Murray, C. R. Kagan. The Effects of Post-Synthesis Processing on CdSe Nanocrystals and their Solids: Correlation Between Surface Chemistry and Optoelectronic Properties. *J. Phys. Chem. C* **118**, 27097-27105 (2014).

"We thank the U.S. Department of Energy Office of Basic Energy Sciences, Division of Materials Science and Engineering under award no. DE-SC0002158 for support of NC synthesis, TEM, and EDX spectroscopy."

C30. J.M.P. Martirez, S. Kim, E.H. Morales, B.T. Diroll, M. Cargnello, T. R. Gordon, C.B. Murray, D.A. Bonnell, A.M. Rappe. Synergistic Oxygen Evolving Activity of a TiO_2-rich Reconstructed $SrTiO_3$(001) Surface. *J. Am. Chem. Soc.*, **137**, 2939-2947 (2015).

"B.T.D. was supported by the US DOE, Office of Basic Energy Sciences, Materials Sciences and Engineering Division, award no. DE-SC0002158."

C31. T. Paik, B. T. Diroll, C. R. Kagan,and C. B. Murray, Binary and Ternary Superlattices Self-Assembled from Colloidal Nanodisks and Nanorods, *J. Am. Chem. Soc,* **137**, 6662-6669 (2015).

"Synthesis of CdSe/CdS dot-in-rods, small- and wide-angle X-ray characterizations, and X-ray simulation were supported by the U.S. Department of Energy Office of Basic Energy Sciences, Division of Materials Science and Engineering under Award No. DE-SC0002158."

C32. S.J. Oh, C. Uswachoke, T. Zhao, J-H. Choi, B. T. Diroll, C. B. Murray, C. R. Kagan, Selective p- and n-Doping of Colloidal PbSe Nanowires To Construct Electronic and Optoelectronic Devices, *ACS Nano* **9**, 7536 (2015).

"We thank the U.S. Department of Energy Office of Basic Energy Sciences, Division of Materials Science and Engineering, under Award DE-SC0002158 for nanowire synthesis."

C33. M. Cargnello, A. C. Johnston-Peck, B. T. Diroll, E. Wong, B. Datta, D. Damodhar, V. T. Doan-Nguyen, A. A. Herzing, C. R. Kagan, C. B. Murray, Substitutional doping in nanocrystal superlattices, *Nature*, **524**, 450 (2015).

…. "secondary support from the US Department of Energy Office of Basic Energy Sciences, Division of Materials Science and Engineering (award number DE-SC0002158) for the development of the semiconductor nanocrystal chemistry and the characterization of electrical conductivity."

C34. F. S. Stinner, Y. Lai, D. B. Straus, B. T. Diroll, D. K. Kim, C. B. Murray, C. R. Kagan, Flexible, High-Speed CdSe Nanocrystal Integrated Circuits, *Nano Lett*. **15**, 7155−7160 (2015).

"We thank the U.S. Department of Energy Office of Basic Energy Sciences, Division of Materials Science and Engineering, under Award No. DE-SC0002158 for NC synthesis."

C35. J.-H. Choi, H. Wang, S. J. Oh, T. Paik, P. S. Jo, J. Sung, X. Ye, T. Zhao, B. T. Diroll, C. B. Murray, C. R. Kagan, Exploiting the colloidal nanocrystal library to construct electronic devices, *Science* **352**, 6282 (2016).

"Indium and CdSe NC synthesis was supported by the U.S. Department of Energy, Office of Basic Energy Sciences, Division of Materials Science and Engineering, under award no. DE-SC0002158."

C36. O. E. Semonin, G. A. Elbaz, D. B. Straus, T. D. Hull, D. W. Paley, A. M. van der Zande, J. C. Hone, I. Kymissis, C. R. Kagan, X. Roy, J. S. Owen, Limits of Carrier Diffusion in n-Type and p-Type $CH_3NH_3PbI_3$ Perovskite Single Crystals, *J. Phys, Chem. Lett*, **7**, 3510-3518 (2016).

"TRMC measurements are supported by the U.S. Department of Energy Office of Basic Energy Sciences, Division of Materials Science and Engineering, under Award DE-SC0002158."

C37. T. Zhao, E. D. Goodwin, J. Guo, H. Wang, B. T. Diroll, C. B. Murray, C. R. Kagan, Advanced Architecture for Colloidal PbS Quantum Dot Solar Cells Exploiting a CdSe Quantum Dot Buffer Layer, *ACS Nano*, **10**, 9267-9273 (2016).

"CdSe QD synthesis and SEM and EDX characterization were supported by the U.S. Department of Energy Office of Basic Energy Sciences, Division of Materials Science and Engineering, under Award No. DE-SC0002158."

C38. D. B. Straus, S. Hurtado Parra, N. Iotov, J. Gebhardt, A. M. Rappe, J. E. Subotnik, J. M. Kikkawa, C. R. Kagan, Direct Observation of Electron−Phonon Coupling and Slow Vibrational Relaxation in Organic−Inorganic Hybrid Perovskites, *J. Am. Chem. Soc*, 138, 13798-13801 (2016).

"Picosecond TRPL is supported by the U.S. Department of Energy, Office of Basic Energy Sciences, under award DE-SC0002158."

C39. T. Paik, J. Yun, B. Fleury, S.-H. Hong, P. S. Jo, Y. Wu, S. J. Oh, M. Cargnello, H. Yang, C. B. Murray, C. R. Kagan, Hierarchical Materials Design by Pattern Transfer Printing of Self-Assembled Binary Nanocrystal Superlattices, *Nano Lett.* ASAP DOI: 10.1021/acs.nanolett.6b04279 (2017).

"GISAXS measurement and analysis was supported by the U.S. Department of Energy, Office of Basic Energy Sciences, Division of Materials Science and Engineering under Award No. DE-SC0002158."

C40. G. A. Elbaz, D. B. Straus, O. E. Semonin, T. D. Hull, D. W. Paley, P. Kim, J. S. Owen, C. R. Kagan, X. Roy, Unbalanced Hole and Electron Diffusion in Lead Bromide Perovskites. *Nano Lett.* **17**, 1727-1732 (2017).

"TRMC measurements are supported by the U.S. Department of Energy Office of Basic Energy Sciences, Division of Materials Science and Engineering, under Award No. DE-SC0002158."

C41. H. J. Yun, T. Paik, B. Diroll, M. E. Edley, J. B. Baxter, and C. B. Murray, "Nanocrystal Size-Dependent Efficiency of Quantum Dot Sensitized Solar Cells in the Strongly Coupled CdSe Nanocrystals/TiO2 System", ACS Appl. Mater. Interfaces, **8** (23), 14692–14700, (2016).

"Secondary support for QD synthesis and characterization was provided by the U.S. Department of Energy Office of Basic Energy Sciences, Division of Materials Science and Engineering (Award DE-SC0002158)."

C42. C. L. Poyser, T. Czerniuk, A. Akimov, B. T. Diroll, E. A. Gaulding, A. S. Salasyuk, A. J. Kent, D. R. Yakovlev, M. Bayer, and C. B. Murray, "Coherent Acoustic Phonons in Colloidal Semiconductor Nanocrystal Superlattices", ACS Nano, **10** (1), 1163–1169 (2016).

"The work was partially supported by the Department of Energy, Office of Basic Sciences, Division of Materials Science (Award No. DE-SC0002158)."

REFERENCES:

(1) Chen, Z.; Moore, J.; Radtke, G.; Sirringhaus, H.; O'Brien, S. Binary Nanoparticle Superlattices in the Semiconductor-Semiconductor System: CdTe and CdSe. *J. Am. Chem. Soc.* **2007**, *129* (50), 15702–15709.

(2) Ou, L. H.; Peng, X. G.; Qu, L. Control of Photoluminescence Properties of CdSe Nanocrystals in Growth. *J. Am. Chem. Soc.* **2002**, *124* (9), 2049–2055.

(3) Turk, M. E.; Vora, P. M.; Fafarman, A. T.; Diroll, B. T.; Murray, C. B.; Kagan, C. R.; Kikkawa, J. M. Ultrafast Electron Trapping in Ligand-Exchanged Quantum Dot Assemblies. *ACS Nano* **2015**, *9* (2), 1440–1447.

(4) Turk, M. E.; Choi, J.-H.; Oh, S. J.; Fafarman, A. T.; Diroll, B. T.; Murray, C. B.; Kagan, C. R.; Kikkawa, J. M. Gate-Induced Carrier Delocalization in Quantum Dot Field Effect Transistors. *Nano Lett.* **2014**, *14* (10), 5948–5952.

(5) Kim, D. K.; Lai, Y.; Diroll, B. T.; Murray, C. B.; Kagan, C. R. Flexible and Low-Voltage Integrated Circuits Constructed from High-Performance Nanocrystal Transistors. *Nat. Commun.* **2012**, *3*, 1216.

(6) Diroll, B. T.; Greybush, N. J.; Kagan, C. R.; Murray, C. B. Smectic Nanorod Superlattices Assembled on Liquid Subphases: Structure, Orientation, Defects, and Optical Polarization. *Chem. Mater.* **2015**, *27* (8), 2998–3008.

(7) Murray, C. B.; Sun, S.; Gaschler, W.; Doyle, H.; Betley, T. A.; Kagan. Colloidal Synthesis of Nanocrystals and Nanocrystal Superlattices. *IBM J. Res. Dev.* **2001**, *45* (1), 47–56.

(8) Cho, K.-S.; Talapin, D. V; Gaschler, W.; Murray, C. B. Designing PbSe Nanowires and Nanorings through Oriented Attachment of Nanoparticles. *J. Am. Chem. Soc.* **2005**, *127* (19), 7140–7147.

(9) Gaulding, E. A.; Diroll, B. T.; Goodwin, E. D.; Vrtis, Z. J.; Kagan, C. R.; Murray, C. B. Deposition of Wafer-Scale Single Component and Binary Nanocrystal Superlattice Thin Films Via Dip-Coating. **2015**, submitted.

(10) Oh, S. J.; Berry, N. E.; Choi, J. H.; Gaulding, E. A.; Paik, T.; Hong, S. H.; Murray, C. B.; Kagan, C. R. Stoichiometric Control of Lead Chalcogenide Nanocrystal Solids to Enhance Their Electronic and Optoelectronic Device Performance. *ACS Nano* **2013**, *7* (3), 2413–2421.

(11) Oh, S. J.; Berry, N. E.; Choi, J.-H.; Gaulding, E. A.; Lin, H.; Paik, T.; Diroll, B. T.; Muramoto, S.; Murray, C. B.; Kagan, C. R. Designing High-Performance PbS and PbSe Nanocrystal Electronic Devices through Stepwise, Post-Synthesis, Colloidal Atomic Layer Deposition. *Nano Lett.* **2014**, *14* (3), 1559–1566.

(12) Dong, A.; Chen, J.; Oh, S. J.; Koh, W.; Xiu, F.; Ye, X.; Ko, D.; Wang, K. L.; Kagan, C. R.; Murray, C. B.; et al. Multiscale Periodic Assembly of Striped Nanocrystal Superlattice on a Liquid Surface. *Nano Lett.* **2011**, *11* (2), 841–846.

(13) Koh, W.; Saudari, S. R.; Fafarman, A. T.; Kagan, C. R.; Murray, C. B. Thiocyanate-Capped PbS Nanocubes: Ambipolar Transport Enables Quantum Dot Based Circuits on a Flexible Substrate. *Nano Lett.* **2011**, *11* (11), 4764–4767.

(14) Oh, S. J.; Wang, Z.; Berry, N. E.; Choi, J.-H.; Zhao, T.; Gaulding, E. A.; Paik, T.; Lai, Y.; Murray, C. B.; Kagan, C. R. Engineering Charge Injection and Charge Transport for High Performance PbSe Nanocrystal Thin Film Devices and Circuits. *Nano Lett.* **2014**, *14* (11), 6210–6216.

(15) Reifsnyder, D. C.; Ye, X.; Gordon, T. R.; Song, C.; Murray, C. B. Three-Dimensional Self-Assembly of Chalcopyrite Copper Indium Diselenide Nanocrystals into Oriented Films. *ACS Nano* **2013**, *7* (5), 4307–4315.

(16) Talapin, D. V; Lee, J.-S.; Kovalenko, M. V; Shevchenko, E. V. Prospects of Colloidal Nanocrystals for Electronic and Optoelectronic Applications. *Chem. Rev.* **2010**, *110* (1), 389–458.

(17) Law, M.; M Luther, J.; Song, Q.; K Hughes, B.; L Perkins, C.; J Nozik, A. Structural, Optical, and Electrical Properties of PbSe Nanocrystal Solids Treated Thermally or with Simple Amines. *J. Am. Chem. Soc.* **2008**, *130* (18), 5974–5985.

(18) Jeong, K. S.; Tang, J.; Liu, H.; Kim, J.; Schaefer, A. W.; Kemp, K.; Levina, L.; Wang, X.; Hoogland, S.; Debnath, R.; et al. Enhanced Mobility-Lifetime Products in PbS Colloidal Quantum Dot Photovoltaics. *ACS Nano 6* (1), 89–99.

(19) Nag, A.; Kovalenko, M. V; Lee, J.-S.; Liu, W.; Spokoyny, B.; Talapin, D. V. Metal-Free Inorganic Ligands for Colloidal Nanocrystals: S(2-), HS(-), Se(2-), HSe(-), Te(2-), HTe(-), TeS(3)(2-), OH(-), and NH(2)(-) as Surface Ligands. *J. Am. Chem. Soc.* **2011**, *133* (27), 10612–10620.

(20) Ning, Z.; Ren, Y.; Hoogland, S.; Voznyy, O.; Levina, L.; Stadler, P.; Lan, X.; Zhitomirsky, D.; Sargent, E. H. All-Inorganic Colloidal Quantum Dot Photovoltaics Employing Solution-Phase Halide Passivation. *Adv. Mater.* **2012**, *24* (47), 6295–6299.

(21) Fafarman, A. T.; Koh, W.; Diroll, B. T.; Kim, D. K.; Ko, D.-K.; Oh, S. J.; Ye, X.; Doan-Nguyen, V.; Crump, M. R.; Reifsnyder, D. C.; et al. Thiocyanate-Capped Nanocrystal Colloids: Vibrational Reporter of Surface Chemistry and Solution-Based Route to Enhanced Coupling in Nanocrystal Solids. *J. Am. Chem. Soc.* **2011**, *133* (39), 15753–15761.

(22) Liu, Y.; Tolentino, J.; Gibbs, M.; Ihly, R.; Perkins, C. L.; Liu, Y.; Crawford, N.; Hemminger, J. C.; Law, M. PbSe Quantum Dot Field-Effect Transistors with Air-Stable Electron Mobilities above 7 cm(2) V(-1) S(-1.). *Nano Lett.* **2013**, *13* (4), 1578–1587.

(23) Zhang, H.; Hu, B.; Sun, L.; Hovden, R.; Wise, F. W.; Muller, D. A.; Robinson, R. D. Surfactant Ligand Removal and Rational Fabrication of Inorganically Connected Quantum Dots. *Nano Lett.* **2011**, *11* (12), 5356–5361.

(24) Fafarman, A.; Koh, W.; Diroll, B. Thiocyanate Capped Nanocrystal Colloids: A Vibrational Reporter of Surface Chemistry and a Solution-Based Route to Enhanced Coupling in Nanocrystal Solids. *J. Am. Chem. Soc.* **2011**, *133* (39), 15753–15761.

(25) Oh, S.; Wang, Z.; Berry, N.; Choi, J. Engineering Charge Injection and Charge Transport for High Performance PbSe Nanocrystal Thin Film Devices and Circuits. *Nano Lett.* **2014**, *14* (11), 6210.

(26) Koleilat, G.; Levina, L.; Shukla, H.; Myrskog, S. Efficient, Stable Infrared Photovoltaics Based on Solution-Cast Colloidal Quantum Dots. *ACS Nano* **2008**, *2* (5), 833–840.

(27) Oh, S. J.; Straus, D. B.; Zhao, T.; Choi, J.-H.; Lee, S.-W.; Gaulding, E. A.; Murray, C. B.; Kagan, C. R.; Kagan, C. R.; Lifshitz, E.; et al. Engineering the Surface Chemistry of Lead Chalcogenide Nanocrystal Solids to Enhance Carrier Mobility and Lifetime in Optoelectronic Devices. *Chem. Commun.* **2017**, *53* (4), 728–731.

(28) Dong, A.; Chen, J.; Vora, P. M.; Kikkawa, J. M.; Murray, C. B. Binary Nanocrystal Superlattice Membranes Self-Assembled at the Liquid-Air Interface. *Nature* **2010**, *466* (7305), 474–477.

(29) Diroll, B. T.; Greybush, N. J.; Kagan, C. R.; Murray, C. B. Smectic Nanorod Superlattices Assembled on Liquid Subphases: Strucutre, Orientation, Defects, and Optical Polarization. **2015**, submitted.

(30) Ye, X.; Chen, J.; Eric Irrgang, M.; Engel, M.; Dong, A.; Glotzer, S. C.; Murray, C. B. Quasicrystalline Nanocrystal Superlattice with Partial Matching Rules. *Nat. Mater.* **2016**, *16* (2), 214–219.

(31) Gaulding, E. A.; Diroll, B. T.; Goodwin, E. D.; Vrtis, Z. J.; Kagan, C. R.; Murray, C. B. Deposition of Wafer-Scale Single-Component and Binary Nanocrystal Superlattice Thin Films Via Dip-Coating. *Adv. Mater.* **2015**, *27* (18), 2846–2851.

(32) Choi, J. H.; Fafarman, A. T.; Oh, S. J.; Ko, D. K.; Kim, D. K.; Diroll, B. T.; Muramoto, S.; Gillen, J. G.; Murray, C. B.; Kagan, C. R. Bandlike Transport in Strongly Coupled and Doped Quantum Dot Solids: A Route to High-Performance Thin-Film Electronics. *Nano Lett.* **2012**, *12* (5), 2631–2638.

(33) Oh, S. J.; Kim, D. K.; Kagan, C. R. Remote Doping and Schottky Barrier Formation in Strongly Quantum Confined Single PbSe Nanowire Field-Effect Transistors. *ACS Nano* **2012**, *6*, 4328–4334.

(34) Moreels, I.; Fritzinger, B.; Martins, J. C.; Hens, Z. Surface Chemistry of Colloidal PbSe Nanocrystals. *J. Am. Chem. Soc.* **2008**, *130* (45), 15081–15086.

(35) Leschkies, K. S.; Kang, M. S.; Aydil, E. S.; Norris, D. J. Influence of Atmospheric Gases on the Electrical Properties of PbSe Quantum-Dot Films. *J. Phys. Chem. C* **2010**, *114* (21), 9988–9996.

(36) Kim, David K; Lai, Y.; Vemulkar, T. R.; Kagan, C. R. Flexible, Low-Voltage, and Low-Hysteresis PbSe Nanowire Field-Effect Transistors. *ACS Nano* **2011**, *DOI: 10.10* (Xx).

(37) Jones, R. H. The Effect of Oxygen on an Evaporated PbSe Layer. *Proc. Phys. Soc. Sect. B* **1957**, *70* (7), 704–708.

(38) Luther, J. M.; Pietryga, J. M. Stoichiometry Control in Quantum Dots: A Viable Analog to Impurity Doping of Bulk Materials. *ACS Nano* **2013**, *7* (3), 1845–1849.

(39) Boneschanscher, M. P.; Evers, W. H.; Geuchies, J. J.; Altantzis, T.; Goris, B.; Rabouw, F. T.; van Rossum, S. A. P.; van der Zant, H. S. J.; Siebbeles, L. D. A.; van Tendeloo, G.; et al. Long-Range Orientation and Atomic Attachment of Nanocrystals in 2D Honeycomb Superlattices. *Science (80-.).* **2014**, *344* (6190), 1377–1380.

(40) Baumgardner, W. J.; Whitham, K.; Hanrath, T. Confined-but-Connected Quantum Solids via Controlled Ligand Displacement. *Nano Lett.* **2013**, *13* (7), 3225–3231.

(41) Diroll, B. T.; Doan-Nguyen, V. V. T.; Cargnello, M.; Gaulding, E. A.; Kagan, C. R.; Murray, C. B. X-Ray Mapping of Nanoparticle Superlattice Thin Films. *ACS Nano* **2014**, *8* (12), 12843–12850.

(42) Diroll, B. T.; Gogotsi, N.; Murray, C. B. Statistical Description of CdSe/CdS Dot-in-Rod Heterostructures Using Scanning Transmission Electron Microscopy. *Chem. Mater.* **2016**, *28* (10), 3345–3351.

(43) Diroll, B. T.; Gaulding, E. A.; Kagan, C. R.; Murray, C. B. Spectrally-Resolved Dielectric Functions of Solution-Cast Quantum Dot Thin Films. *Chem. Mater.* **2015**, *27* (18), 6463–6469.

(44) Diroll, B. T.; Koschitzky, A.; Murray, C. B. Tunable Optical Anisotropy of Seeded CdSe/CdS Nanorods. *J. Phys. Chem. Lett.* **2014**, *5* (1), 85–91.

(45) Diroll, B. T.; Murray, C. B. High-Temperature Photoluminescence of CdSe/CdS Core/shell Nanoheterostructures. *ACS Nano* **2014**, *8* (6), 6466–6474.

(46) Paik, T.; Ko, D.-K.; Gordon, T. R.; Doan-Nguyen, V.; Murray, C. B. Studies of Liquid Crystalline Self-Assembly of GdF_3 Nanoplates by in-Plane, out-of-Plane SAXS. *ACS Nano* **2011**, *5* (10), 8322–8330.

(47) Fafarman, A. T.; Koh, W.; Diroll, B. T.; Kim, D. K.; Ko, D.-K.; Oh, S. J.; Ye, X.; Doan-Nguyen, V.; Crump, M. R.; Reifsnyder, D. C.; et al. Thiocyanate-Capped Nanocrystal Colloids: Vibrational

Reporter of Surface Chemistry and Solution-Based Route to Enhanced Coupling in Nanocrystal Solids. *J. Am. Chem. Soc.* **2011**, *133* (39), 15753–15761.

(48) Garc'ia-Santamar'ia, F.; Brovelli, S.; Viswanatha, R.; Hollingsworth, J. A.; Htoon, H.; Crooker, S. A.; Klimov, V. I. Breakdown of Volume Scaling in Auger Recombination in CdSe/CdS Heteronanocrystals: The Role of the Core-Shell Interface. *Nano Lett.* **2011**, *11* (2), 687–693.

(49) Keene, J. D.; Mcbride, J. R.; Orfield, N. J.; Rosenthal, S. J.; Al, K. E. T. Elimination of Hole À Surface Overlap in Graded CdS X Se 1 À X Nanocrystals Revealed by Ultrafast Fluorescence Upconversion Spectroscopy. **2014**.

(50) Choi, J.-H.; Oh, S. J.; Lai, Y.; Kim, D. K.; Zhao, T.; Fafarman, A. T.; Diroll, B. T.; Murray, C. B.; Kagan, C. R. In Situ Repair of High-Performance, Flexible Nanocrystal Electronics for Large-Area Fabrication and Operation in Air. *ACS Nano* **2013**, *7* (9), 8275–8283.

(51) Klimov, V. I.; McBranch, D. W.; Leatherdale, C. A.; Bawendi, M. G. Electron and Hole Relaxation Pathways in Semiconductor Quantum Dots. *Phys. Rev. B - Condens. Matter Mater. Phys.* **1999**, *60* (19), 13740–13749.

(52) Klimov, V. I. Spectral and Dynamical Properties of Multiexcitons in Semiconductor Nanocrystals. *Annu. Rev. Phys. Chem.* **2007**, *58*, 635–673.

(53) Sewall, S. L.; Cooney, R. R.; Anderson, K. E. H.; Dias, E. A.; Kambhampati, P. State-to-State Exciton Dynamics in Semiconductor Quantum Dots. *Phys. Rev. B - Condens. Matter Mater. Phys.* **2006**, *74* (23), 235328.

(54) Sewall, S. L.; Cooney, R. R.; Kambhampati, P. Experimental Tests of Effective Mass and Atomistic Approaches to Quantum Dot Electronic Structure: Ordering of Electronic States. *Appl. Phys. Lett.* **2009**, *94* (2009).

(55) Straus, D. B.; Hurtado Parra, S.; Iotov, N.; Gebhardt, J.; Rappe, A. M.; Subotnik, J. E.; Kikkawa, J. M.; Kagan, C. R. Direct Observation of Electron–Phonon Coupling and Slow Vibrational Relaxation in Organic–Inorganic Hybrid Perovskites. *J. Am. Chem. Soc.* **2016**, *138* (42), 13798–13801.

(56) Geyer, S.; Porter, V.; Halpert, J.; Mentzel, T.; Kastner, M.; Bawendi, M. Charge Transport in Mixed CdSe and CdTe Colloidal Nanocrystal Films. *Phys. Rev. B* **2010**, *82* (15).

(57) Luther, J. M.; Law, M.; Beard, M. C.; Song, Q.; Reese, M. O.; Ellingson, R. J.; Nozik, A. J. Schottky Solar Cells Based on Colloidal Nanocrystal Films. *Nano Lett.* **2008**, *8* (10), 3488–3492.

(58) Turk, M. E.; Choi, J.; Oh, S. J.; Fafarman, A. T.; Diroll, B. T.; Murray, C. B.; Kagan, C. R.; Kikkawa, J. M. Gate-Induced Carrier Delocalization in Quantum Dot Field E Ff Ect Transistors. *Nano Lett.* **2014**, *14*, 5948−5952.

(59) Houtepen, A. J.; Kockmann, D.; Vanmaekelbergh, D. Reappraisal of Variable-Range Hopping in Quantum Dot Solids. *Nano Lett.* **2008**, *8*, 3516.

(60) Goodwin, E. D.; Straus, D. B.; Gaulding, E. A.; Murray, C. B.; Kagan, C. R. The Effects of Inorganic Surface Treatments on Photogenerated Carrier Mobility and Lifetime in PbSe Quantum Dot Thin Films. *Chem. Phys.* **2015**.

(61) Zhitomirsky, D.; Voznyy, O.; Hoogland, S.; Sargent, E. H. Measuring Charge Carrier Diffusion in Coupled Colloidal Quantum Dot Solids. *ACS Nano* **2013**, *7* (6), 5282–5290.

(62) Straus, D. B.; Goodwin, E. D.; Gaulding, E. A.; Muramoto, S.; Murray, C. B.; Kagan, C. R. Increased Carrier Mobility and Lifetime in CdSe Quantum Dot Thin Films through Surface Trap Passivation and Doping. *J. Phys. Chem. Lett.* **2015**, *6* (22), 4605–4609.

(63) Semonin, O. E.; Elbaz, G. A.; Straus, D. B.; Hull, T. D.; Paley, D. W.; van der Zande, A. M.; Hone, J. C.; Kymissis, I.; Kagan, C. R.; Roy, X.; et al. Limits of Carrier Diffusion in *N* -Type and *P* -Type $CH_3NH_3PbI_3$ Perovskite Single Crystals. *J. Phys. Chem. Lett.* **2016**, *7* (17), 3510–3518.

(64) Elbaz, G. A.; Straus, D. B.; Semonin, O. E.; Hull, T. D.; Paley, D. W.; Kim, P.; Owen, J. S.; Kagan, C. R.; Roy, X. Unbalanced Hole and Electron Diffusion in Lead Bromide Perovskites. *Nano Lett.* **2017**, *17* (3), 1727–1732.

(65) Koh, W.; Saudari, S. R.; Fafarman, A. T.; Kagan, C. R.; Murray, C. B. Thiocyanate-Capped PbS Nanocubes: Ambipolar Transport Enables Quantum Dot Based Circuits on a Flexible Substrate. *Nano Lett.* **2011**, *11* (11), 4764–4767.

(66) Choi, J.-H.; Fafarman, A. T.; Oh, S. J.; Ko, D.; Kim, D. K.; Diroll, B. T.; Muramoto, S.; Gillen, J. G.; Murray, C. B.; Kagan, C. R.; et al. Band-like Transport in Strongly-Coupled and Doped Quantum Dot Solids: A Route to High-Performance Thin-Film Electronics. *Submitted* **2012**.

(67) Diroll, B. T.; Gordon, T. R.; Gaulding, E. A.; Klein, D. R.; Paik, T.; Yun, H. J.; Goodwin, E. D.; Damodhar, D.; Kagan, C. R.; Murray, C. B. Synthesis of N-Type Plasmonic Oxide Nanocrystals and the Optical and Electrical Characterization of Their Transparent Conducting Films. *Chem. Mater.* **2014**, *26* (15), 4579–4588.

(68) Fafarman, A. T.; Hong, S.-H.; Caglayan, H.; Ye, X.; Diroll, B. T.; Paik, T.; Engheta, N.; Murray, C. B.; Kagan, C. R. Chemically Tailored Dielectric-to-Metal Transition for the Design of Metamaterials from Nanoimprinted Colloidal Nanocrystals. *Nano Lett.* **2013**, *13* (2), 350–357.

(69) Fafarman, A. T.; Hong, S.-H.; Oh, S. J.; Caglayan, H.; Ye, X.; Diroll, B. T.; Engheta, N.; Murray, C. B.; Kagan, C. R. Air-Stable, Nanostructured Electronic and Plasmonic Materials from Solution-Processable, Silver Nanocrystal Building Blocks. *ACS Nano* **2014**, *8* (3), 2746–2754.